TECHNO SCIENTIFIC INC.
205 Champagne Drive, Downsview, Ontario M3J 2C6 (416) 635-7626, Telex 06-986766 TOR

DEVELOPMENT OF PORTABLE TEST EQUIPMENT EMPLOYING ULTRASONIC PULSE-ECHO TECHNIQUE TO DETERMINE FLAWS IN CONCRETE

Final Report

by

Techno Scientific Inc.

Work on this project was conducted under the auspices of the Canada Centre for Mineral and Energy Technology, Energy, Mines and Resources Canada.

DSS FILE NUMBER: 23SQ.23440-4-9249
DSS CONTRACT SERIAL NUMBER: 0SQ84-00270
CANMET SCIENTIFIC AUTHORITY: Mr. V. Malhotra

69 pp

March 1986

Prepared by: M. Macecek

MICROMEDIA

TABLE OF CONTENTS

1. INTRODUCTION 1

2. STATE OF THE ART SURVEY 2

2.1 Scattering of Ultrasound in Polycrystalline Bodies.. 5

3. PREPARATION OF SAMPLES 7

4. EXPERIMENTAL 8

4.1 Velocity 8
4.2 Attenuation 9
4.3 Acoustic Impedance and Diffraction Testing 9

4.3.1 Air Entrainments 9

5. TRANSDUCER DESIGN AND OPTIMIZATION 10

6. EVALUATION OF COUPLING 12

7. EVALUATION OF EXISTING PULSERS 13

8. MEASUREMENTS OF ULTRASONIC VELOCITY 14

8.1 Transmit Receive VS Pulse Echo 14
8.2 Effect of Aggregate Size 15

9. MEASUREMENTS OF ULTRASONIC ATTENUATION 16

9.1 Frequency Dependence of Attenuation 16
9.2 Absorption 16

9.2.1 Shift in Frequency Spectrum VS Path Length .. 17

9.3 Acoustic Impedance Effects 17

9.3.1 Scattering 17
9.3.2 Air Entrainments 18
9.3.3 Reinforced Concrete 18

10. FIELD EXPERIMENTS 20

10.1 Signal Response from Water-Filled Cracks 20
10.2 Detecting Air Voids or Cracks with 45° Angle Transducers 20
10.3 Detection and Sizing of Cracks 21
10.4 Monitoring of a Visible Crack 21
10.5 Characterization of Depth and Length of Cracks 22
10.6 Monitoring of Depth and Length of Cracks 23

11. DATA ACQUISITION AND SIGNAL PROCESSING 25

12. DISCUSSION 27

13. CONCLUSIONS 28

ACKNOWLEDGEMENT 28

REFERENCES 29

TABLES

FIGURES

APPENDIX A - SURVEY OF COMMERCIALLY AVAILABLE INSTRUMENTATION

APPENDIX B - SPECIFICATIONS FOR THE PORTABLE UNIT

MEASUREMENTS OF ULTRASONIC VELOCITY AND ATTENUATION

1. INTRODUCTION

The overall objective of this work is the development of a state of the art prototype of a portable ultrasonic concrete tester with pulse-echo capabilities. The report describes Phase I of the work, addressing general background research. The data compiled in this work helps to define the development of the instrument, which will be the subject of Phase II of this project.

The work was carried out in three main thrusts:

- development of an ultrasonic transducer with high penetrating power to serve as transmitter, and a highly sensitive transducer as receiver;
- development of a hard pulser with 1000V pulse;
- measurements on concrete samples in laboratory structures as well as in the field to determine ultrasonic attenuation, velocities, damping, scattering and mode conversion in concrete.

Of paramount importance was the study of pulse-echo or pitch and catch techniques with access from one side. This is the most important objective since the majority of engineering structures offer access from one side only. Existing commercial equipment is inadequate in large structures such as offshore drilling platforms, dams, and nuclear power installations.

We have succeeded in developing both hard pulser and high sensitivity transducers which, when combined with the narrow band filtered amplifier, gave penetrating capabilities of about 40 ft (larger than 13m) from one side. The modules were tested in the field and evidence is presented to support the above claim.

2. STATE OF THE ART SURVEY

Nondestructive inspection of concrete is relatively recent. It is used to determine strength, thickness, presence of foreign objects, cracks and degradation caused by chemical attack or fire (1,2,3).

While ultrasonics is a well established technique in the inspection of metals (4), its extension to concrete was delayed because of inherent difficulties. The earliest reported ultrasonic work was carried out by Leslie and Cheesman in 1949 (5), and simultaneously by Jones (6). Progress was slow due to the poor availability of optimized transducers and support electronics. Advances in new ceramic materials (7,8) provided a basis for a much more efficient conversion. Ultrasonics in concrete benefited from the research in rock mechanics and geological activities (9,10).

Instruments available typically address the velocity of sound only. Several units are commercially available, and are listed in the Appendix. They provide digital indications of the time of flight (TOF) from which velocity can be determined. The majority of applications are carried out in a transmit-receive mode

(Figure 1), where access from both sides of the sample is required. Laboratory measurements reported use an oscilloscope to monitor the shape of the pulse. A typical block diagram is shown in Figure 2. A number of studies addressed the relationship between compressive strength of concrete and its ultrasonic pulse velocity (11,12,13,14). Generally, the relationship is not unique, as it is a function of age of concrete, moisture, type of aggregate to matrix ratio, amount of steel reinforcement, etc. In combination with other methods such as rebound number, the method can lead to more accurate results. The problem is not in the accuracy of velocity measurements, but in the uncertain relationship between velocity and other properties of concrete.

Estimating concrete strength in a water saturated condition by pulse velocity alone is unreliable and impractical. The strength of concrete can be determined better by using two acoustic properties i.e., pulse velocity, which represents elastic properties, and a damping constant which represents the inelastic properties (15).

In addition to strength measurements, a need for thickness monitoring led to the development of the pulse-echo (P-E) method and resonance method. The resonance method was found to be impractical for field use, while the P-E method gave 3% accuracy in 90% of cases (16). However, the instrument was cumbersome. Very low frequencies were used (200-600Hz) by mechanical impact. The reflection from cracks 100m away were detected (17).

Unlike metals, when the surface of concrete is isonified by a piston source a number of modes exist. Figure 3 illustrates the three dominant components, i.e. surface wave, compressional or longitudinal wave, and shear wave. The relationships at the boundary are given by the usual refraction expression:

$$\frac{C_1}{\sin\alpha} = \frac{C_2}{\sin\beta} \qquad [1]$$

The surface wave component is always present, and this prevents measurements on thin walls from one side. An optimum transducer can shorten the ringing time of each mode but this is frequently done at the expense of sensitivity. Figure 4 illustrates the use of wedges to circumvent the problem of surface waves.

For laboratory studies, immersion coupling or full immersion testing is possible with the advantage of choosing the proper refracted angle or wave mode. Surface waves which are considered detrimental in contact testing can be used to monitor cracks at the surface (18). Surface waves propagating along solid-liquid interface are continuously radiated at critical angles into the liquid. The critical angle is given as

$$\theta = \sin^{-1} \frac{C_L \text{ (liquid)}}{C_S \text{ (solid)}} \qquad [2]$$

For water-concrete interface, the critical angle is 40°. When the ultrasonic beam encounters a crack or other discontinuity, a significant reflection of energy occurs. In addition, a mode conversion at the interface may occur. For normal incidence the amount of energy is given by:

$$R = \frac{\left(\frac{Z_1}{Z_2} - \frac{Z_2}{Z_1}\right)^2}{4 \cot^2 \frac{2\pi d}{\lambda_2} + \left(\frac{Z_1}{Z_2} + \frac{Z_2}{Z_1}\right)^2} \qquad [3]$$

Z (acoustic impedance) = ρ

$Z = \rho \times V$
d = width of crack
λ = wavelength of radiation in air or water

A considerable difference in reflected signal in air filled and water filled cracks can be explained with the help of this equation, and experiments will be discussed in Section 10.

2.1 Scattering of Ultrasound in Polycrystalline Bodies

When an ultrasonic beam propagates through a solid polycrystaline body, the amplitude decays exponentially. When the beam is reflected by a reflector, the amplitude of the reflected wave, C, can be expressed as:

$$C = C_o (\lambda x, rw, Sp, Sn) \exp.^{-\alpha . r} \qquad [4]$$

where C_o is a function of wavelength, λ directionality diagram of the probe and reflector, Sp is the probe area, Sn reflector area, α is the attenuation factor and r the travelled distance. The attenuation factor α (or extinction coefficient) is made up of the scattering and absorption factors

$$\alpha = \alpha + \alpha_a \qquad [5]$$

In polycrystalline materials (such as concrete) the scattering factor is believed to be dominant.

The scattering of ultrasound was investigated by Merkulov (19) and reviewed by Papadakis (20). Since the model is based on isotropic elastic properties of metals, the conclusions could be altered by the strong elastic and structural anisotropies of concrete.

The dominant parameter in the ultrasonic attenuation (A) is the radio D/λ, i.e., grain diameter vs wavelength. The dividing line is drawn at $\lambda = 2\pi D$. For the $\lambda > 2\pi D$, the dependence can be expressed as

$$A \sim B_1 + B_2 f^2 + A_o D \qquad [6]$$

For the region $\lambda \cong 2\pi D$ the dependence is quadratic

$$A \sim D \cdot f^2 \qquad [7]$$

and for the $\lambda < 2\pi D$

$$A_o \sim B_1 f + A_1 D^3 f^4 \qquad [8]$$

where the B_1 and B_2 represent the elastic hysteresis and thermoelastic losses, D is the grain size, A_o and A_1 are independent constants.

For example, at f = 40kHz, the wavelength of the longitudinal and shear waves in concrete are λ_L= 4-8cm, λ_S= 2-4cm.

We have, therefore, a region of quadratic and a region of quadric dependence of ultrasonic attenuation on frequency, suggesting the use of low frequencies for coarse polycrystalline materials. For any given frequency, longitudinal waves should have a lower attenuation due to their longer wavelength.

Another treatment of scattering was given by Sayers and Smith (21). They theoretically predicted velocities in porous concrete.

3. PREPARATION OF SAMPLES

Investigations were carried out on samples prepared by TSI and other organizations to establish an accurate test procedure. Measurements were augmented by trials on field structures. The dimensions and velocities of different samples are given in Table I. These types of samples included large concrete slabs, small slabs and small cylinder beams. The samples were selected for their variation in concrete density, porosity, aggregate type, size, and cement composition. Their aggregate size and description are given in Table II.

Samples were also prepared in house using normal Portland cement, CSA type 10. The aggregates included fine grain sand and crushed limestone or gravelstone up to 3.2cm in size. The dimensions of these samples are given in Table III. Small and large aggregate samples (2G and 2H respectively) were prepared for testing the effect of scattering of the wave. Small aggregates measured 1.1cm and larger aggregates measured 3.2cm. These concrete samples had, for each one, the same aggregate cement ratio by volume.

The samples used for testing of air voids and cracks included samples 2B and 2I. Sample 2B was a 34.8cm x 15.9cm x 5cm concrete slab containing air voids measuring 1.6cm and 0.8cm in thickness and cracks measuring approximately 10cm x 5cm, and 5cm

x 6cm. Test sample 2I contained air voids measuring 6cm x 5cm x 3.7cm and 5.5cm x 3cm x 2.5cm.

In addition to laboratory samples, we were given access to field structures with thicknesses of up to 13m (40ft), and varying degrees of concrete quality. Included were cracks, internal cavities, reinforcing bars, repaired cracks, and weathered surface layers.

4. EXPERIMENTAL

Transit times for each sample were measured using the PUNDIT (Portable Ultrasonic Nondestructive Digital Indicating Tester) generator to compare concrete density with velocity and attenuation. Also, a laboratory setup using TSI instrumentation was employed with superior performance to that of the Pundit. The setup consisted of a pulser, receiver and a time counter, giving accuracies of up to 10 us.

As shown in Table IV, two transit times were measured to calculate the average pulse velocity for each sample at 37 kHz and a pulse setting of 500 volts.

4.1 Velocity

For the pulse velocity measurements shown in Table I, a higher pulse velocity was observed for the sample of highest density.

4.2 Attenuation

The greater attenuation of the wave was observed for the sample of lower density. Figure 5 depicts two concrete samples (1C and 1G). Sample 1G is of high and sample 1C is of low density. The received waveform from 1C was measured at 244mV at a transit time distance of only 5.7cm. The higher density sample revealed less attenuation at 2.44V for a longer transit time distance of 20cm.

Velocity and the rate of attenuation were tested for different concrete samples with varying low frequency transducers, and the shift in frequency spectrum of the received signal was related to the thickness of the sample tested. Absorption losses were also observed to increase with increase in frequency of the transducer used.

4.3 Acoustic Impedance and Diffraction Testing

4.3.1 Air Entrainments

The effects of air gaps and cracks on velocity and attenuation and characteristics of the received waveform (both transmit-receive and pulse-echo modes) were analyzed. A frequency analysis of the received waveform was observed to determine the size and location of the flaws.

5. TRANSDUCER DESIGN AND OPTIMIZATION

Ultrasonic transducers are a vital but poorly understood element in the ultrasonic detection chain. Properties of transducers used in the inspection of concrete are critical. Each inspection method requires a different type of transducer. A transducer converts an electrical pulse or burst into a mechanical wave. it is a highly linear device, i.e. the strain is proportional to electric charge and conversely, strain produces electric charges in the receiving mode. A schematic construction of a transducer is illustrated in Figure 6, showing components of a normal transducer. Each geometry requires an optimal transducer. The parameters of interest are:

- near field length
- beam spread
- impedance
- damping
- frequency
- sensitivity
- refracted angle
- casing

The near field beam size which is related to frequency determines the resolving power of the system (22). The beam has two regions:

i) a near-field (Fresnel zone) extending from the crystal out to the "near-field point" at about $D^2/4\lambda$, where D is the piezoelectric disc's diameter and the wavelength. Over this length the beam necks down to a minimum average width of about 0.6D. The intensity is a maximum at the near-field point.

ii) A far-field (Fraunhofer zone) extending from the near-field point out to infinity. Here the beam diverges into a cone whose semi-angle is about arcsin (λ/D), which is typically .5 degrees. Thus the beam width increases and the intensity drops according to the inverse square law.

Immersion testing uses mostly far field. Contact testing involves both near and far fields.

A wide range of angles are used to cover the whole volume of concrete objects. In contact testing the transducer is usually attached to a plexiglass wedge which defines the refracted angle of a transducer. These angles are typically 35, 45, 60 and 70 degrees. A design of an angled probe is shown in Figure 7 with examples of a contact probe and coupling wedges. The beam produced by the transducer is determined by standard techniques (23,24,25) and is usually defined both in water (0 degree transducer) and in the test piece examined.

In concrete testing, the frequencies used are much lower than in metal NDT applications. Typical frequencies are in the 20 to 200 kHz range, with some at 500 to 1000 kHz for thickness monitoring. Since penetrating power is of paramount importance crystal stacking is employed, with crystals electrically in parallel and mechanically in series to increase the amplitude of the pulse. Some TSI designed transducers for concrete inspection are shown in Figure 8.

If a separate transmitter can be used, an inexpensive casing is utilized. If the same transducer acts as a receiver, an inner metallic shielding is required. Alternatively, stainless steel casing is employed. The transducer should be internally tuned with electrical impedance set to 50-100 ohms in order to be compatible with existing pulsers. An example of an impedance chart of some concrete transducers is shown in Figure 9. In

addition to impedance matching, an electrical damping circuit (low Q tank inductance) can be used (26), tuned to the thickness mode resonant frequency of the crystal. This shortens the dead zone of the transducer, and limits lateral oscillations in the crystals. The impedance chart depicted in the above figures can be used to measure the quality of transducers. The beam spread is governed by the standard equation below, and the sensitivity can be measured using loop sensitivity numbers or hydrophones (27).

$$\sin \theta = \frac{1.22V}{nd}$$

where θ = semi angle
V = velocity of longitudinal waves in the medium
d = diameter of the transmitter
n = integer

6. EVALUATION OF COUPLING

The efficient transfer of acoustical energy from the transducer to the test piece and back is essential. Since the transducer and the test piece are not acoustically matched, a portion of energy is reflected back to the transducer. The amount of energy transfered is given by the ratio of acoustic impedances. In order to improve energy transfer between the transducer and test piece, a matching layer is inserted between the transducer and medium. A number of papers address the question of the impedance matching layer, which is a geometrical mean between the acoustic impedances of the transducer and test piece face (25,27).

To evaluate the transfer of energy from the transducer to the test piece, experimentation was carried out with different

mediums such as thin rubber (single and multilayer), water, dry air, oil (H68 machining oil), Industrial Ultrasonic Couplant Gel and white lithium grease at 47 kHz and a pulse voltage of 400V. The results are shown in Table V.

The outcome of the tests indicate that the machining oil provided the best coupling by obtaining a received signal amplitude of 700mV peak to peak, followed by water which produced a peak to peak amplitude of 420mV. The gel provided a lower received signal amplitude in the order of 170mV. The signals obtained from using these three types of coupling methods were far superior to those found by using rubber or air coupling. The lithium grease gave good results and was superior to the gel.

Liquid buffer coupling was also experimented with. A plexiglass wedge was milled to allow for a layer of couplant about 1cm thick, then feeding and bleeding holes to insert couplant into this layer. The layer was sealed with a rubber liner. This local immersion coupling was used in the field on weathered concrete structures which had coarse surfaces. Both water and antifreeze were used as couplant. The design of the wedge is detailed in Figure 10.

7. EVALUATION OF EXISTING PULSERS

An investigation of a pulser which was developed by the Hughes Aircraft Co. (28), was carried out. This pulser gave a pulse output of 1000V and delivered it into a 50 ohm load. The circuit developed a very narrow pulse width in the nanosecond range with a typical rise time of 8 nanoseconds. The peak current output

was 20 amps. However, the narrow pulse does not give enough energy to excite the concrete transducers, as the energy is given by the integral under the curve.

The PUNDIT generator was developed specifically for concrete testing. The display indicates the wave transit time in microseconds. The transmitter delivers a 1000 volt pulse at 1.5 microseconds and a pulse repetition frequency (PRF) of 8-10pps. into a 50 ohm load. When measured, the voltage on transducers reached only 700-800 volts.

The evaluation of the above pulsers led to the conclusion that a new pulser 'hard' enough to penetrate more than 10m of concrete had to be developed.

8. MEASUREMENTS OF ULTRASONIC VELOCITY

8.1 Transmit-Receive vs Pulse-Echo

Velocity and attenuation of elastic waves are the most relevant attributes pertaining to the nondestructive testing of concrete. Acoustic velocity is dependent on the parameters of density, porosity, aggregate type, void size and cement composition, whereas the attenuation of sound is influenced by the absorption, scattering, acoustic impedance effects and diffraction of the ultrasonic wave. The test data analyzed in this report has been taken from a number of velocity and attenuation measurements of concrete.

For the direct transmission method, the time for the pulse to travel from the transmitting to the receiving transducer is measured.

The pulse-echo method uses the same surface for mounting both the pulse source and the receiving transducer. Material defects or interfaces of different densities or mismatched impedances within the concrete structure will determine the characteristics of the reflected echoes (29,30,31).

8.2 Effect of Aggregate Size

Since the modulus of elasticity and density of coarse aggregates in concrete are considerably higher than those of the binding mortar matrix, the mortar has a lower specific acoustic impedance than the coarse aggregate. The mismatch in acoustic impedances will cause excessive scattering of the soundwave if the wavelength is less that the mean size of the aggregate.

Scattering is reduced when the impedance of mortar reaches that of the aggregate. Samples 2G and 2H with small and large aggregates were tested through frequency analysis to determine whether aggregates can be distinguished. Measurements were carried out at 47kHz with a 400V pulse using the Krautkramer KB6000 flaw detector.

Results revealed that large aggregate size yields larger signal amplitude with negligible frequency shift of transmitted signals, up to a difference of 6dB (50%) between coarse and fine aggregate signals.

9. MEASUREMENTS OF ULTRASONIC ATTENUATION

9.1 Frequency Dependance of Attenuation

The attenuation of the ultrasonic wave as a function of path for a range of low frequency transducers (47 kHz, 65 kHz and 87 kHz respectively) was measured (Table VIII). With a pulse voltage of 400V, it was observed that for longer wavelengths the loss in acoustic pressure with increase in path length was smaller.

Frequency content of the propagating pulse was also affected by attenuation. With an increase in path length the higher frequency components of the wave were attenuated more heavily.

Figure 11 reveals an increase in attenuation for an increase in path length depending on the frequency of the transducers. The frequency spectrum depended greatly on the input frequency of transducers as observed from the variations in attenuation, amplitude range and in the spectral components received.

9.2 Absorption

Absorption or damping of the ultrasonic wave is mostly caused by internal friction from the conversion of mechanical to heat energy. Energy of the wave is reduced with path length since heat flows more slowly than the ultrasonic wave. The penetration power of the wave will also decrease exponentially with path length, depending on the initial acoustic pressure and the attenuation coefficient of the concrete sample (32).

9.2.1 Shift in Frequency Spectrum vs Path Length

The frequency spectrum of samples 2C and 2F revealed a 0.6 dB attenuation of the pulse for a 10.9 cm increase in path length. The applied pulse of 400V was taken from the Krautkramer KB6000 unit and the receiving transducer was connected to the Anritsu Network/Spetrum analyzer MS420B. The 65 kHz transducer was used. The shift of the frequency spectrum peaks to the lower range was observed at 2.7 kHz when measuring the 1.32 MHz component. A shift in the frequency spectrum of a concrete sample is more evident for a significant increase in path length.

To investigate the change in spectral component peaks with change in path length, the change in amplitude for each component was recorded for samples 2C and 2F. Two 47 kHz transducers were used. The results listed in Table VI showed that, for both tests, a significant increase in dB amplitude was obtained for components between 600 kHz and 860 kHz for an 8.8cm increase in path length.

9.3 Acoustic Impedance Effects

9.3.1 Scattering

Scattering of the ultrasonic wave is due to sample acoustic discontinuities which deflect small amounts of ultrasonic energy. These boundaries also produce a difference in acoustic velocity and acoustic impedance. The extent of scattering is dependent on the ratio of grain size to ultrasonic wavelength of the wave and on the physical properties on each side of the boundary (33).

9.3.2 Air Entrainments

The effects of acoustic impedance occurs from the partitioning of energy when waves are reflected at the various interfaces within a test material. Such an energy loss occurs for discontinuities that are present within a concrete structure. When an ultrasonic wave travels through the interface of one medium to another, the difference in acoustic impedance will determine the portion of energy that is reflected, while the remaining energy is transmitted into the second medium.

9.3.3 Reinforced Concrete

To study the velocity as a function of reinforcement, initial tests with sample 1E (see Figure 13) revealed a higher apparent velocity when the steel bar was directly between the transmitting and receiving transducer. The steel bar measured 1.7 cm in diameter and appeared 6.5 cm below the surface of the test piece. Figure 14 shows the smallest transit time measured at 47.6 us. The 65 kHz transducers had a diameter of 2.5 cm. The larger diameter 37 kHz transducers showed little or no change in pulse velocity with the presence of reinforcing steel.

There was a significant change in velocity for a bar diameter comparable with the beam for a path placed perpendicular to the direction of reinforcement.

It was observed from the measured frequency spectrum that the amplitude of most of the components increased with the presence

of the steel bar (the steel bar being directly between the path of the 65 kHz transducers). The pulse velocity measurements of concrete with reinforcement (sample 2A) were higher than that of concrete, both for pulse path perpendicular and parallel to the direction of reinforcement. Influence of the pulse velocity was observed for the wave path parallel to the direction of reinforcement.

Additional CRT pictures with rebars are shown in the following section.

10. FIELD EXPERIMENTS-PULSE ECHO

10.1 Signal Response from Water-Filled Cracks

All experiments detailed were done in the pulse-echo mode. Ultrasonic response was measured from cracks filled with water as compared with air-filled cracks in order to establish the possibility of monitoring water-immersed concrete structures. Data are displayed in Figure 15 showing the geometry of the experiments as well as a plot of obtained data.

The experiments showed that immersed concrete exhibits slightly higher ultrasonic velocity and lower attenuation, resulting in higher amplitudes. This is in agreement with data observed elsewhere (34). The frequency used was 65 kHz with a 1000V pulser designed by TSI. Experiments proved that cracks can be reliably detected when immersed in water. The received crack signal amplitudes, however, are slightly lower (.71dB) than for dry concrete. The impedance change for concrete to air is .413 to 6-10 x 10 vs 1.48 x a0 to 6-10 x 10 kg/m s for concrete-water interface. We have also measured cracks filled with grout and excellent signal levels were obtained.

10.2 Detecting Air Voids or Cracks with 45° Angle Transducers

The objective of this test was to demonstrate the ability to locate voids or discontinuities in concrete. A vertical hole (about 5" in diameter) was first tested as shown in Figure 16a. The hole axis was vertical to the surface. The thickness of the slab was 2 feet. With the transducers inclined at 45°, the

horizontal distance to the reflector is half of the separation between transducers, corrected for the refracted angle, since the distance is a cosine projection of the actual sound path. See Figure 16b. The maximum signal observed from the transducer was 30mVp-p, and peaks were easy to separate. See Figure 16c. The location of the hole was accurate to within .1".

10.3 Detection and Sizing of Cracks

The detection and sizing of cracks is perhaps the most important and and critical application for monitoring of large structures (35,36,37,38,39). The process can be considered twofold, i.e. crack detection and its sizing and orientation. We have carried out a number of experiments on field structures in order to study:

- signal levels reflected by the crack
- blocking of signals in transmit-receive (T-R) mode
- variation of signals as a function of distance from cracks
- influence of wedge angle upon received signal.
- influence of multiple cracking
- influence of quality of concrete
- influence of reinforcing steel

10.4 Monitoring of a Visible Crack

A crack daylighting in the structure was monitored. The distance to the crack was varied, and amplitude and TOF of the ultrasonic signal were monitored. Ultrasonic gel was used as a couplant. The geometry of the set up was identical to Figure 16.

The amplitude of reflected signal increased as transducers were placed closer to the crack (Figure 17). Ringing in the echo signal also increased with shorter sound path.

10.5 Characterization of Depth and Length of Cracks

Wedge angles of 25° and 45° were compared (See Figures 18a and 18b). The 45° wedge angle had a shorter time of flight and larger received signal amplitude. Calculating crack location from maximum compressional wave using 25° and 45° wedges, the maximum recorded TOF for transducer separation of 72 cm was: 779us for 45° wedges; 993us for 25° wedges. At a velocity of 1.75mm/us, this gives a distance of 136cm for the 45° wedge and 173cm for the 25° wedge.

We also examined the crack in structure believed to be more than 20 feet from the surface. The crack was reliably detected from the front face at different heights. Signals obtained with the help of a filtered amplifier were excellent (see Figure 19). The crack deviated slightly from the vertical as revealed by measurements at different heights. The existence of the crack and its location were verified by subsequent core drilling. Its distance from the edge of the structure was within 6" from the data predicted by ultrasonics. The agreement between coring and ultrasonics can be considered very good, since precise ultrasonic velocity could not be established at the location of the crack. The coring also revealed that the crack was very wide (over 2cm) at this location. This gave rise to very strong ultrasonic reflections, as depicted in Figure 19.

10.6 Monitoring of Depth and Multiple Cracks

Additional experiments were carried out using TSI laboratory instrumentation on structures 40 feet or more in depth which contained cracking. Some cracks were visible on the surface. All measurements were done in the pulse-echo mode from one side only. A series of figures (20a-d) depict typical CRT rf waveform signals containing a surface wave signal, which is always present and saturates the amplifier. Following this, one or more echoes from cracks or other reflectors can be observed. The signal to noise ratio is very high and the location of the crack can be accurately determined. The presence of the surface wave signal creates the problem of the so-called "dead zone". The actual length of the surface wave pulse prevents any echo to be discerned within this time interval (Figure 21). If thinner structures are to be inspected, either the power of the pulser must be reduced or the use of wedges must be incorporated as reported in Section 5. From Figure 22, a crack cannot be detected in this geometry in the first 3 feet of concrete. However, there were instances of shallow cracks which could be seen within the envelope of a surface wave pulse.

The question of multiple crack detection is also addressed. Measurements were carried out in localities where multiple cracking was observed. Figure 20b indicates two cracks at depths of 9 and 15 feet respectively. This indicates that ultrasonics can be discerned even though the amplitude of the echo signal from the crack shielded by the crack closer to the surface is

low. In general, the rf waveforms of crack signals could be very sharp and strong even if an additional crack exists between the surface and crack being monitored (Figure 20c).

Depending on the orientation and morphology of the crack, the rf response can vary from sharp, narrow spikes (Figure 20d) to much wider, long ringing echo shapes. One could optimize signals by selective filtering and/or attenuation of the echo (40,41,42).

A series of indicated flaws and signals were measured in an "old" concrete structure. Such structures had higher signal to noise (S/N) ratio and frequently higher attenuation. Figures 23a and 23b show the ultrasonic monitoring of newer structures. Electrical cleanliness i.e. high S/N ratio, is evident in these figures. Also noticeable are narrower echo signals, indicating a more planar nature of the reflector, i.e. crack, and less scattering of sound in the structure. This is evident in the near vertical rising edge of the echo signal. Large concrete structures are frequently filled with reinforcing bars. The samples in Figures 24a,b,c show ultrasonic indications of reinforcing bars evenly spaced within the structure.

In general, both longitudinal and perpendicular reinforcement bars can be detected if of sufficient size (1-2") (43,44).

11. DIGITAL DATA ACQUISITION AND SIGNAL PROCESSING

In order to use some advanced signal processing techniques, the digitization of signals was incorporated. Initial experiments on digital data acquisition and signal processing were carried out using a 20 MHz digitizer and a system available at TSI (45). The 20 MHz analog-to-digital converter digitizes and stores 4096 points of an analog input signal. RF waveforms of sample 1L were digitized at various sampling rates of 20 MHz, 5 MHz and 2.5 MHz, by dividing the base sampling rate (20 MHz) by 1, 4 and 8 respectively. A block diagram of the setup is shown in Figure 25. The transducers used were 47 kHz.

The difference observed between the RF waveforms of Figures 26 and 27, both digitized at a sampling rate of 2.5 MHz, is a result of signal averaging. Signal averaging involves the digitization and summation of sampled RF waveforms. The summation of these waveforms divided by the number of samples taken eliminates or cancels out random noise while the signal increases, thus improving the signal to noise ratio (S/N).

The received signal is sampled and stored in memory at a time after the negative going edge of the trigger. A repetitive trigger, and successive data acquisition, is controlled by software for the signal averaging process.

The digitized waveform of Figure 27 shows the high attenuation of sample 2H, which contained large aggregates. The summation of 64 samples divided by a factor of 4 produced a magnification of 16

times. The same magnification with no signal averaging, shown in Figure 20, reveals a much lower signal to noise ratio. The signal summation offers an elegant way of improving the capabilities of the instrument brought about by changes in chip technology.

12. DISCUSSION

The experimental work, as well as the literature search revealed that pulse-echo instrumentation for concrete inspection can be improved upon. We have received clean signals after reflection from 40 foot walls, i.e. a total sound path of over 80 feet. Experiments also revealed the importance of optimized transducers. A variety of transducers should be made available in a wide frequency range (from 30kHz to 1MHz) including an array of elements for increased penetration power. The transducers devised by TSI offered higher sensitivity and better signal to noise ratios at different frequencies. It may be beneficial to devise a separate transmitter and receiver with different characteristics. The literature supports our finding (46-51)

Ultrasonic pulsing of at least 1000V was also developed. However, for some applications, tone burst lower voltage pulsing may be more advantageous. On the receiving electronics, the design of selectively tuned active filters resulted in an improvement in range by a factor of 4. We believe that piezoelectric pulsers are superior to mechanical ones as in (52).

While many tasks were handled by an operator, it is believed that a microprocessor menu-driven CPU will be required to optimize setting of the instrument, speed the evaluation of results and provide advanced signal process techniques combined with a permanent record of data. A CRT screen is considered absolutely essential, allowing the operator to interact with instruments according to his best judgement. A proposed feature

of the instrument to be addressed in Phase II can be found in Appendix B. Many other applications can be successfully handled if the instrument has the properties listed above (53-62).

13. CONCLUSIONS

The work carried out in this project indicates that greatly improved pulse-echo instrumentation based on existing techniques can be offered. With optimized transducers, powerful pulser, low noise active filtered amplifiers, data digitization and storage, a new breed of sophisticated but portable instrument can be built to provide the performance and permanent record as require today.

ACKNOWLEDGEMENT

We wish to acknowledge Mr. V.M. Malhotra of CANMET, Energy, Mines and Resources for his guidance, suggestions and genuine interest in the project.

We would also like to thank Mr. S. Fassula of TROW Ltd. for test samples, and Mr. J. Strycek of NDT Technologies of Montreal for useful suggestions and the loan of some instrumentation.

REFERENCES

1. T.N. Claytor, W.A. Ellingson, "Development of Ultrasonic Methods for the Nondestructive Inspection of Concrete", Ultrasonics 1983 Symposium Proceedings, Halifax, N.S.

2. H. N. Tomsett, "The Practical Use of Ultrasonic Pulse Velocity Measurements in the Assessment of Concrete Quality", Magazine of Concrete Research (London), V.32, no. 110, Mar. 1980, pp.7-16.

3. D.G. Watkeys, "Nondestructive Testing of concrete Subject to Fire Attack", MSc. (Eng.) Thesis, University of London, 1977.

4. J. Krautkramer, H. Krautkramer, Ultrasonic Testing of Materials, Springer-Verlag, New York 1969.

5. J.R. Leslie, W.J. Cheesman, "An Ultrasonic Method of Studying Deterioration and Cracking in Concrete Structure", J. Am. Concr. Inst., 46:9:17-36; 1949.

6. R. Jones, "The Nondestructive Testing of Concrete", Mag. Concr. Res; London, 1:2:67-78; 1949.

7. W.A. Smith, A.A. Shaulov, B.M. Singer, "Properties of Composite Piezoelectric Materials for Ultrasonic Transducers", 1984 Ultrasonics Symposium, Dallas.

8. M. H. Slayton, P. A. Angleton, W. Janicky, "Correlation Between Physical Dimensions and Piezoelectric Parameters for Poled Ferroelectric Disks", 1984 Ultrasonics Symposium, Dallas.

9. O.L. Anderson, R.C. Liebermann, "Sound Velocities in Rocks and Minerals: Experimental Methods, Extrapolations to Very High Pressures, and Results", Physical Acoustics, Ed. W.P. Mason, Academic Press, New York (1968), V.IV, Part B, p.329.

10. L. Knopoff, "Attenuation of Elastic Waves in the Earth", Physical Acoustics, Ed. W.P. Mason, Academic Press, New York (1965), V III, Part B, p.287.

11. E. A. Whitehurst, "Evaluation of Concrete Properties From Sonic Tests", Am. Concr. Inst. Monograph, No.2; 1966.

12. R. Jones, "Nondestructive Testing of Concrete", London, Cambridge University Press; 1962.

13. M. F. Kaplan, "Compressive Strength and Ultrasonic Pulse Velocity Relationships for Concrete in Columns", J. Am. Concr. Inst; 54:8:675-688; 1958.

14. R. Jones, E.N. Gatfield, "Testing Concrete by an Ultrasonic Pulse Technique", Road Res. Tech. Paper 34, Road Research Laboratory, Crowthorne, London; 1955.

15. A. Galan, "Estimate of Concrete Strength by Ultrasonic Pulse Velocity and Damping Constant", J. Am. Concr. Inst. 64:10:678-684; 1967.

16. R. Muenow, "A Sonic Mehtod to Determine Pavement Thickness", Journal of the PCA Research and Development Laboratories, Vol.5, No. 3, Sept 1963; p 8-21.

17. K. Nand, et. al. "A Sonic Method for the Detection of Deep Cracks in Large Structures", Indian Concrete Journal, March 1974; p 98-102.

18. R. L. Smith, The use of Surface Scanning Waves to Detect Surface-Opening Cracks in concrete", NDT International, Oct 1984; p 273-275.

19. L.G. Merkulov, "Investigation of Ultrasonic Scattering in Metals", Soviet Phys. Tech. Phys., 1, 159 (1956).

20. E.P. Papadakis, "Physical Acoustics and Properties of Solids", Vol AV B, Ed. W.P. Mason, p 269.

21. C. M. Sayers, R.L. Smith, "The Propagation of Ultrasound in Porous Media", Butterworth & Co. (publishers) Ltd.; 0041-624X/82/050201-05.

22. I. Bredael, "Characterization of Ultrasonic Transducers", Research Techniques in Nondestructive Testing III, ed. R.S. Sharpe, CH.5; New York 1977.

23. K. F. Bainton, M.G. Silk, "Some Factors Which Affect the Performance of Ultrasonic Transducerd", Brit.J.Ndt 22 15, 1980.

24. A.S. Birks, "Quantitative Characterization of Ultrasonic NDE Transducers", Proc. 13th Symp. on NDE, NTIAC, Southwest Research Institute, 486 (1981).

25. C. S. Desilets, J.D. Fraser, G.S. Kino, "The Design of Efficient Broadband Piezoelectric Transducers", IEEE Trans. Sonics and Ultra. SU-25, 115; 1978.

26. G. Bradfield, "Determining the Thickness of Concrete Pavements by Mechanical Waves: Directed-beam method", Mag. Conc. Res., V16, no. 46; March 1964.

27. H. Kwun et al., "Ultrasonic Transducers - Performance Variability, Design, and Manufacturing Procedures", NTIAC, Southwest Research Institute, NTIAC-84-1.

28. J. Stover, N. Komatsu, A. Nieto, "Nanosecond Pulsers for mm wave Tubes", Hughes Aircraft Co., HAC-FR79-14-353; Feb 80.

29. O. A. Kayyali, "Using Ultrasonic Pulse Method in Monitoring Concrete Deterioration in Hot Weather", Durability Build Mater. V2 N2, May 1984, p129-138.

30. I.A. Pathan, "Improved Method to Determine the Cracking Stress, Cracking Strain and Young's Modulus of Plain Concrete in Direct Tension", Mehran Univ. Res J Eng Technology, V3 N1, Jan 1984, p 1-6.

31. L. I. Knabe, G. V. Blessing, J.R. Clifton, "Laboratory Evaluation of Ultrasonics for Crack Detection in Concrete", J Am Concr Inst, V80 N1, Jan-Feb 1983, p 17-27.

32. R. Sjoeblom, "Measurements of the Speed of Sound and the Absorption Coefficient for Ion Exchange Resin Embedded in Concrete and Bitumen using Ultrasonic Waves at Around 0.1MHz" Dec 1981, PC A02//MF A01.

33. W. N. Reynolds, S.J. Wilkinson, "Nondestructive Physical Analysis of Concrete", Br. J. Nondestr. Test, Jan 1979,21(1).

34. H. T. Thornton Jr., D. Glass, "Ultrasonic Velocity Measurements in Concrete, Lock and Dam Number 24, Mississippi River, April 1980, Report WES/MP/SL-80-2.

35. W. N. Reynolds, "Measuring Concrete Quality Nondestructively", Br J Nondestr Test, V26 N1, Jan 1984, p 11-14.

36. A.P. Keiller, "Preliminary Investigation of Test Methods for the Assessment of Strength of in Situ Concrete", Cement and Concrete Association, Slough, England; C192, PC E04/MF E04.

37. L. I. Knab, G. V. Blessing, J.R. Clifton, "Laboratory Evaluation of Ultrasonics for Crack Detection in Concrete", Feb 83; American Concrete Institute Jnl., paper No. 80-3.

38. R.L. Stowe, H.T. Thornton Jr., "Condition Survey, Repair and Rehabilitation, Lock and Dam Number 24, Mississippi River", Report TRRL-LR-953.

39. J. R. Clifton, E.D. Anderson, "Nondestructive Evaluation Methods for Quality Acceptance of Hardened Concrete in Structures", Report NBSIR-80-2163.

40. A. M. Alexander, "Development of Procedures for Nondestructive Testing of Concrete Structures. Report 2. Feasibility of Sonic Pulse-echo Technique", April 1980, Report WES-MP-C-77-11-2.

41. V. A. Latyshenko, "Researches on Concrete and Reinforced Concrete", October 1966, Report FTD-TT-65-1701.

42. R. W. McClung, "On Nondestructive Testing in the U.S.A. of Prestressed Concrete Pressure Vessels for Nuclear Reactors", IAEA Panel, Vienna, Nov 1972, p 527-540.

43. H.W. Chung, "Effects of Embedded Steel Bars upon Ultrasonic Testing of Concrete", Mag. Concr. Res. (GB), March 1978, p 19-25.

44. I. I. Vainstok, A. YA. Goikhman, V.S. Yamshchikov, "Ultrasonic Testing of the Strength of Loaded Concrete and Reinforced Concrete Structures", Akust. Zh. (USSR), July-Aug 1976, 22(4), p 336-8.

45. M. Macecek, D.K. Mak, K. Luscott, J. Wells, "Automated Ultrasonic Testing Systems for the Characterization of Defects in Weldments", Fifth Canadian Conference on Nondestructive Testing proceedings, p 66-78.

46. L. Millstein, G. M. Sabnis, "Determination of Concrete Strengths using Ultrasonic Waves", ASCE, New York, 1983, p 561-564.

47. Y. Tanigawa, K. Yamada, S. Kumagai, "Expression for Estimating Compressive Strength of Concrete by Combined Nondestructive Testing Method", Proceedings of the 25th Japan Congress on Materials Research, Tokyo, Oct 1981, p 251-254.

48. R.T.L. Allen, "Alkali-Silica Reaction in Great Britain - A Review", Cem and Concr Assoc, London, 1981; #2 S252/18.

49. H. Achyutha, P. S. Rao, "Assessment of In-situ concrete Strength Results of Some Field Investigations", Am Concr Inst., Maharashtra India Chapter, Bombay, 1981; p 2.25-2.26.

50. K. R. Datye, R.J. Dubhas, S.K. Guha, R.A. Joshi, "Techniques for Inspection of quality and Evaluation of Strength of Concrete, During and After Construction", Proceedings-International Symposium on Rehabilitation of Structures, Bombay India, Dec. 1981; p 17-23.

51. H. Austerlitz, H.R. Carleton, "Precision Intervalometer for the Remote Acquisition of Ultrasonic Data", Oceans (New York), 81 Vl; IEEE (CAT N 81CH1685-7), 1981; p 501-505.

52. N. J. Carino, M. Sansalone, "Pulse-echo Method for Flaw Detection in Concrete", NBS Technical Note 1199, US Department of Commerce.

53. W. N. Reynolds, S.J. Wilkinson, D.C. Spooner, "Ultrasonic Wave Velocities in Concrete", Mag. Concr. Res. (GB); Sept 1978, 30(104), p 139-44.

54. A. M. Filonidov, "Use of Ultrasound for Checking the Frost Resistance of Concrete", Gidrotekh. Stroit., May 1982, p28-31.

55. S. Motooka, M. Okujima, "Study on Detection of Buried Steel Bar in Concrete with Electromagnetic Impact Driving Method", Jpn. J. Appl. Phys., V 21, p 144-6.

56. E. A. Whitehurst, V.M. Malhotra, "Nondestructive Tests", Chapter 15, ASME Special Technical Publication 169B, 1979, p 200-225.

57. V. M. Malhotra, "Testing Hardened Concrete: Nondestructive Methods (Monograph No. 9), ACI Publications 1976.

58. K. S. Law, H.W. Chung, "Ultrasonic Testing of Concrete-The Practical Aspects", Hong Kong Eng., Nov 1981, 9(11); p 45-8.

59. I.S. Ting, "Assessment of Concrete by Nondestructive Means", Thesis, University of Nottingham, England,.

60. J. H. Bungey, "The Validity of Ultrasonic Pulse Velocity Testing of In-place concrete for Strength", NDT International, December 1980; 13(6), p 296-300.

61. H. N. Tomsett, "The Practical Use of ultrasonic Pulse Velocity Measurements in the Assessment of Concrete Quality", Mag. Concr. Res. (GB), March 1980; p 7-16.

62. M. R. Datta, G.K. Anand, "Nondestructive Concrete Analyser", Stud. J. dInst. Electron. and Telecommun. Eng., July 1979, 20(3); p 123-5.

TABLE I

VELOCITIES OF DIFFERENT CONCRETE SAMPLES

SERIES	SIZE OF SPECIMEN (mm)	AVERAGE PULSE VELOCITY (mm/us)
1L	229 x 100 x 26 slab	5.15
1G	200 x 83 cylinder beam	4.76
1E	208 x 100 cylinder beam	4.18
1B	490 x 257 x 88 slab	4.11
1A	300 x 130 x 78.5 slab	4.08
1D	352 x 220 x 80 slab	4.06
1H	115 x 50 x 50 beam	4.01
1K	163 x 50 x 49 beam	3.92
1F	345 x 85 x 82 slab	3.83
1I	380 x 95 x 71 slab	3.78
1C	352 x 139 x 57 slab	3.68

TABLE II

MAXIMUM AGGREGATE SIZE AND DESCRIPTION

SERIES	SIZE (mm)	DESCRIPTION	
		POROSITY	AGGREGATE
1B	0.275	dense	finest
1D	0.620	porous	medium
1G	0.845	very dense	medium
1K	1.255	porous	coarse
1H	1.270	porous	coarse
1F	1.380	porous	coarse
1A	1.465	porous	coarse
1C	1.505	most porous	very course
1I	1.690	porous	coarse
1E	2.465	dense	very coarse
1L	--	most dense	most coarse

TABLE III

DIMENSIONS OF SAMPLES 2A-2J

SERIES	SIZE OF SPECIMEN (mm)
2A	488 X 293 X 77 SLAB
2B	348 X 159 X 50 SLAB
2C	42 X 151 CYLINDER BEAM
2D	56 X 151 CYLINDER BEAM
2E	79 X 151 CYLINDER BEAM
2F	130 X 151 CYLINDER BEAM
2G	80 X 133 CYLINDER BEAM
2H	65 X 150 CYLINDER BEAM
2I	70 X 150 CYLINDER BEAM

TABLE IV

TIME AND ATTENUATION MEASUREMENTS

FOR SAMPLES 1A-1L

SERIES	PULSE PATH LENGTH (cm)	TRANSIT TIME (us)	RECEIVED VOLTAGE (Vp-p)	ATTENUATION (-dB)
1A	13	31.8, 31.6	.44	61.1
	30	75.1, 73.2	.2	67.96
1B	25.7	61.1, 61.4	.102	73.81
	49	123.6, 120.7	.0165	89.63
1C	32.5	87.7, 85.3	.31	64.15
	5.7	16.5, 15.2	.071	76.95
1D	22	52.6, 52	.106	73.47
	35.2	92.6, 87.2	.255	66.94
1E	20.8	51.6, 48.2	.042	81.51
1F	34.5	88.4, 88.2	.18	68.87
	8.2	22.1, 21.5	.142	70.9
1G	20	42.3, 41.7	1.08	53.31
1H	5	12.6, 12.4	10.6	33.47
	11.5	28.7, 28.5	.82	55.70
1I	38	103.6, 98.3	.18	68.87
	71	19.1, 18.5	.124	72.11
IK	4.9	13.2, 13.6	1.48	50.57
	16.3	39.0, 39.0	.84	55.49
1L	2.6	5.5, 4.7	8.4	35.49
		5.3, 4.7		

TABLE V

EVALUATION OF COUPLING BETWEEN

TRANSDUCER AND TEST PIECE

COUPLING	RECEIVED VOLTAGE (mV p-p)
Dry	1
Rubber (1 layer)	3
Rubber (2 layers)	3
Water	420
Oil (H68 Machining Oil)	700
Gel	170
Lithium Grease	300

TABLE VI

MEASUREMENTS OF SPECTRAL COMPONENTS
PATH LENGTH 2C-2F

COMPONENT (kHz)	RECEIVED dB LEVEL PATH LENGTH 2C	PATH LENGTH 2F	CHANGE IN dB LEVEL
TEST 1			
72.00952	7.9	4	-3.9
288.00848	5.7	2.4	-3.3
360.00760	3	0	-3
522.00652	3.5	0	-3.5
600.006	4.2	7.8	+3.6
684.00544	4.3	4	-0.3
738.00508	4.4	7	+2.6
858.00428	1.6	3.3	+1.7
1320.0012	2.1	2.2	+0.1
TEST 2			
79.20956	6.1	4	-2.1
230.40872	5.3	2.9	-2.4
374.40792	4.8	4.8	--
511.20716	4.8	3	-1.8
590.40672	3.5	9.1	+5.6
676.80624	3.4	5.2	+1.8
741.60588	6	10.9	+4.9
856.80524	3.3	6.4	+3.1
1015.20436	1.2	0.8	-0.4
1317.60268	5.2	5.2	--
1432.80204	1.6	2.2	+0.6
1548.0014	2.5	1.8	-0.7

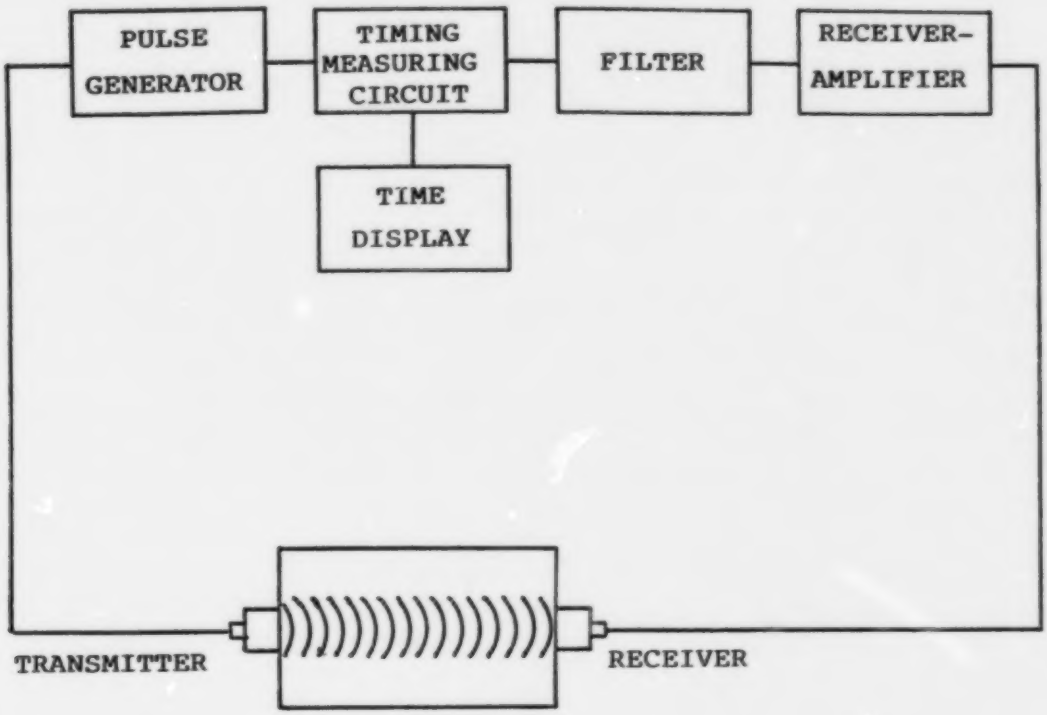

Figure 1. Through-transmission (T-R) method of concrete testing

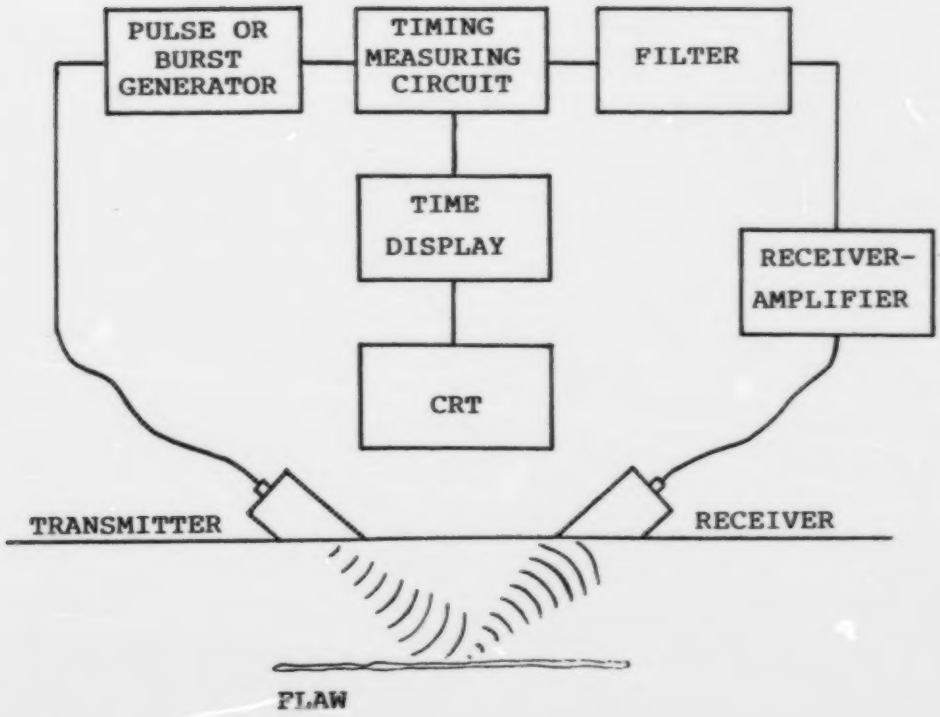

Figure 2. Pulse-echo (P-E) method of concrete testing

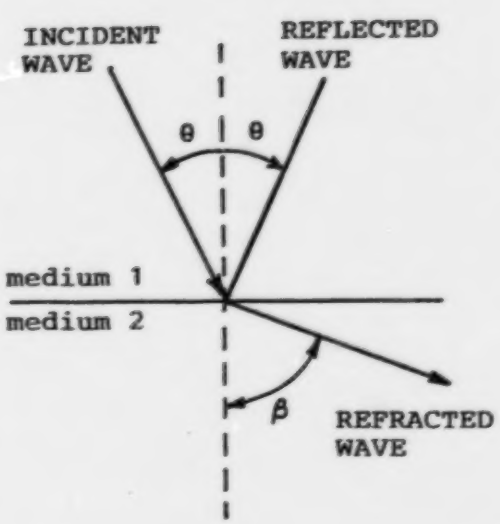

$$\frac{\sin\theta}{C_1} = \frac{\sin\beta}{C_2}$$

a) Reflection and Refraction

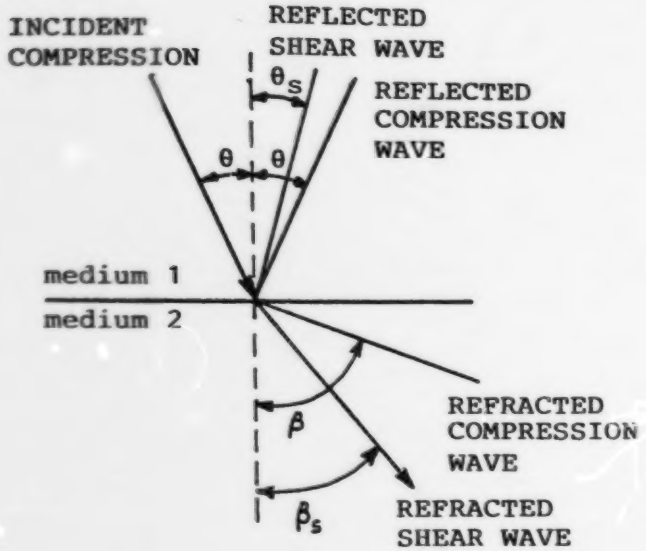

$$\frac{\sin\theta}{C_{p1}} = \frac{\sin\beta}{C_{p2}} = \frac{\sin\theta_s}{C_{s1}} = \frac{\sin\beta_s}{C_{s2}}$$

b) Mode Conversion

Figure 3. Interaction of ultrasonic wave at the surface of concrete

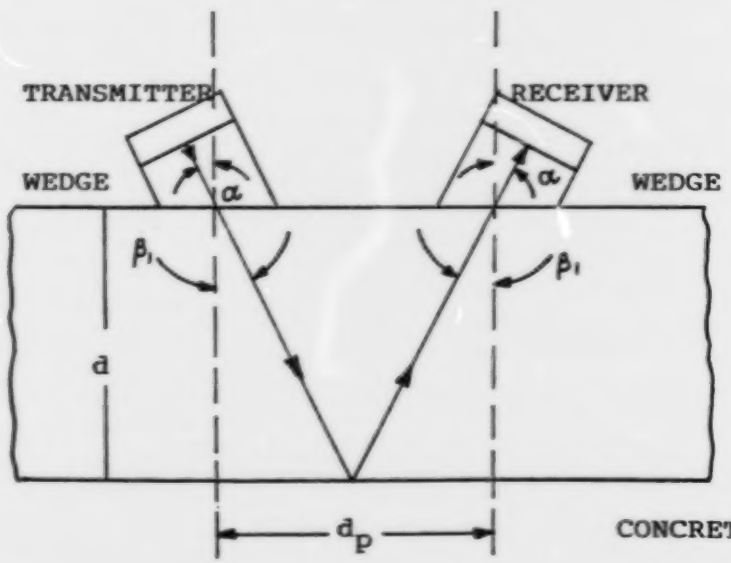

β_1 = refracted angle in concrete
α = angle of incidence
d = thickness of sample
d_p = separation of exit paths of transducers and wedges

Figure 4. Use of wedges to steer the ultrasonic beam into concrete and to minimize surface wave interference

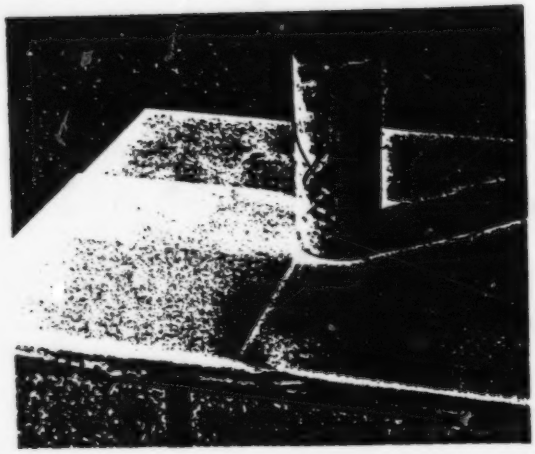

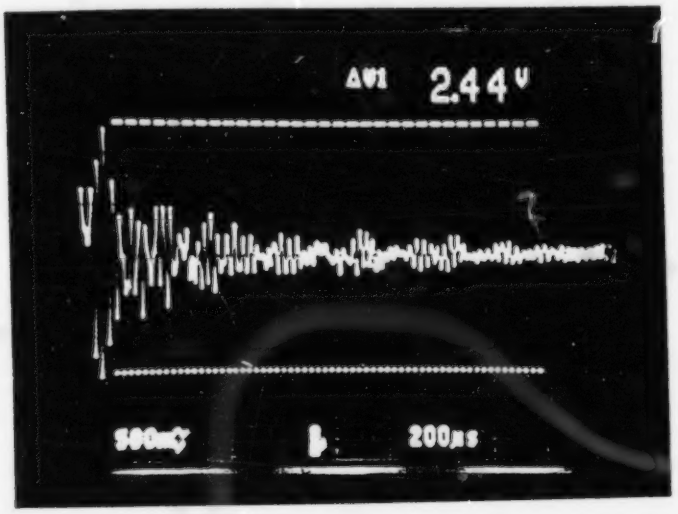

High density sample

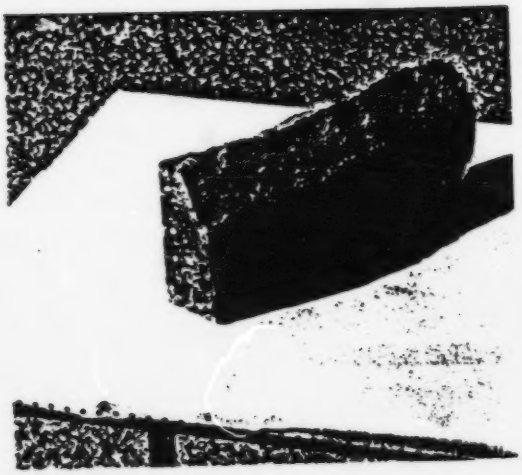

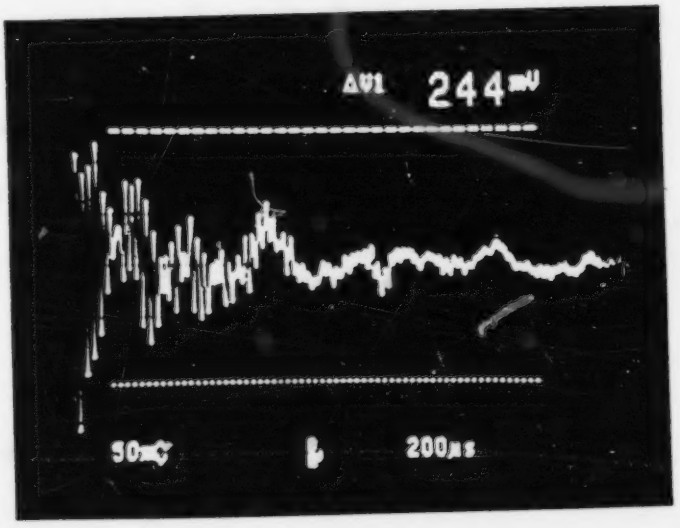

Low density sample

Figure 5. Difference in sound attenuation between high and low density samples

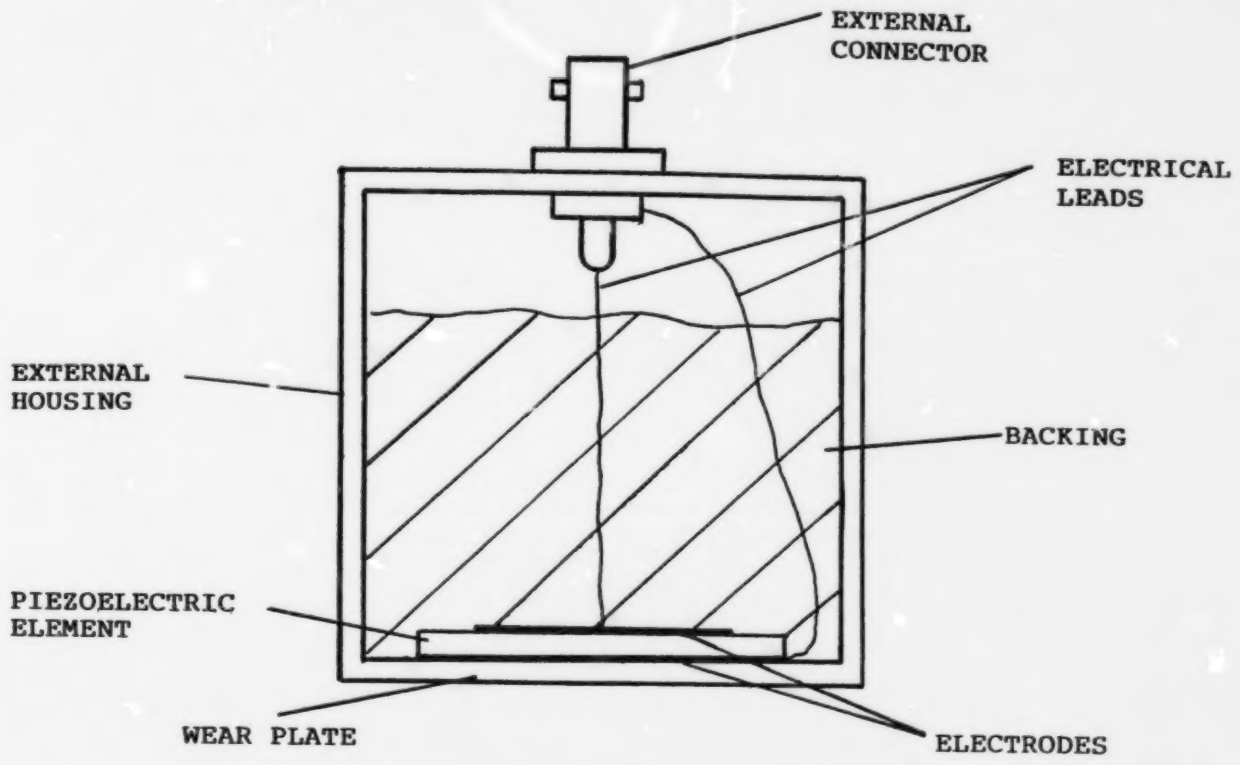

Figure 6. Schematic design of a transducer

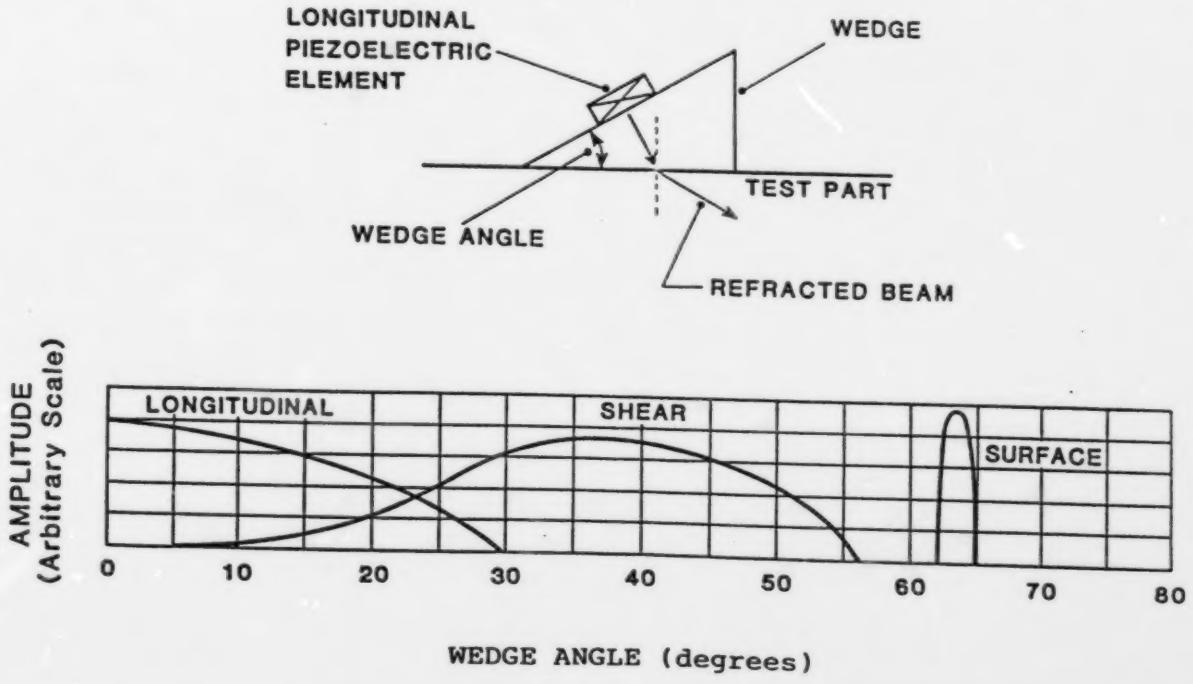

Figure 7. Design of an angle probe and its typical beam profile

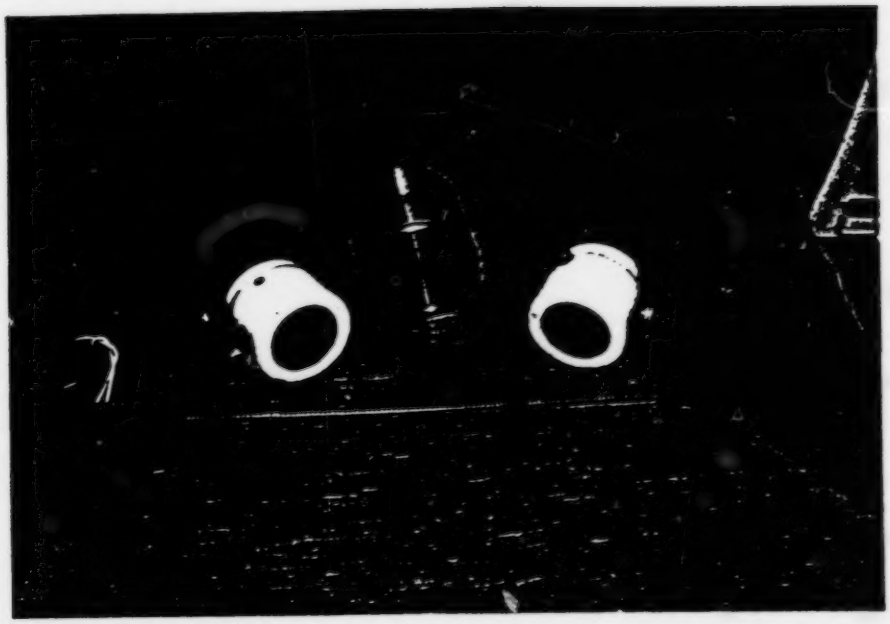

Figure 8 Photo of TSI designed transducer

concrete transducer

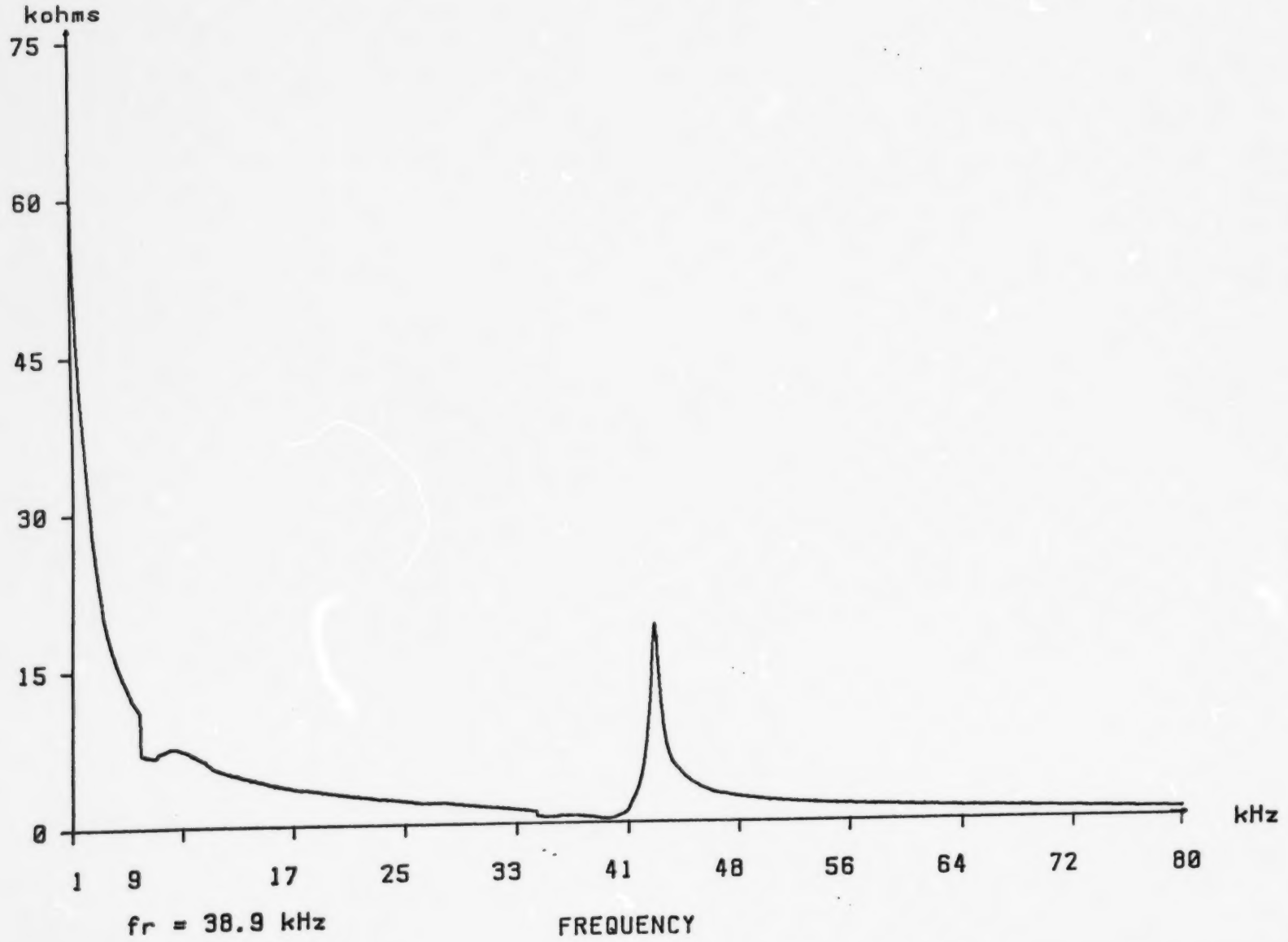

Figure 9. Impedance chart of concrete transducer

Reference # 185

TECHNO SCIENTIFIC INC.

02-11-1986

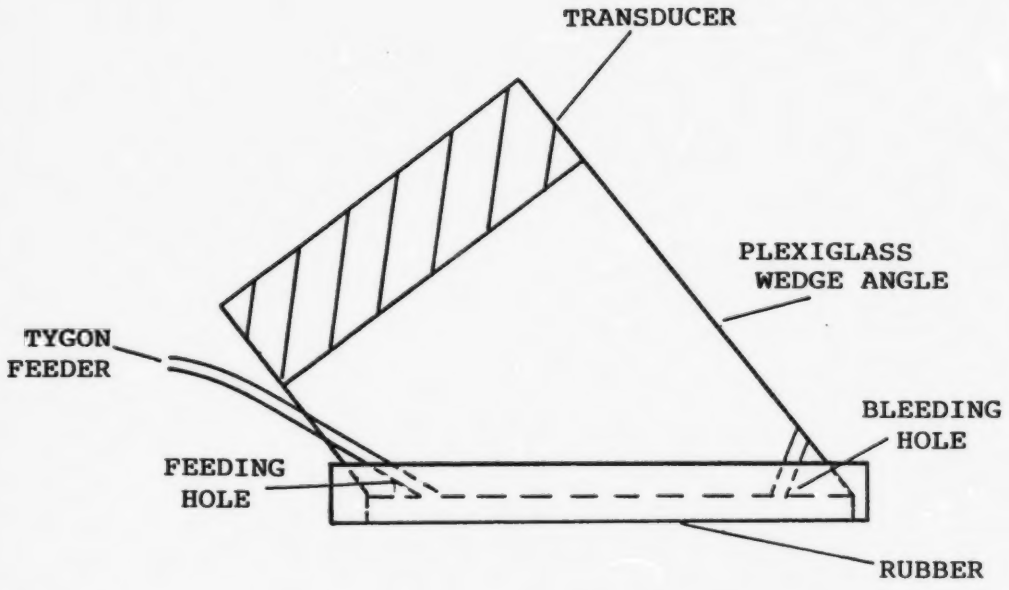

Figure 10. Design of a local immersion transducer (water-filled)

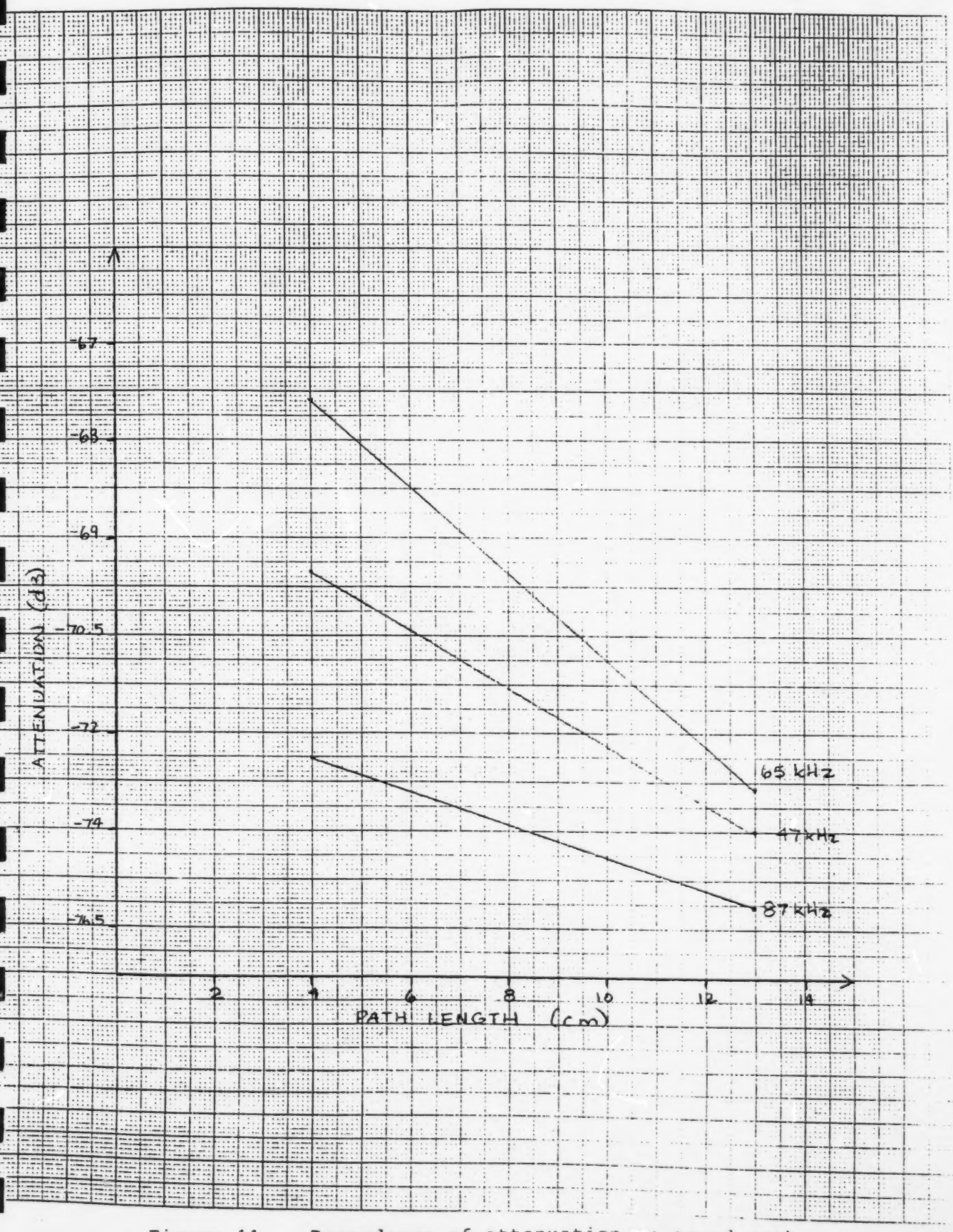

Figure 11 Dependence of attenuation on sound path length for different frequencies

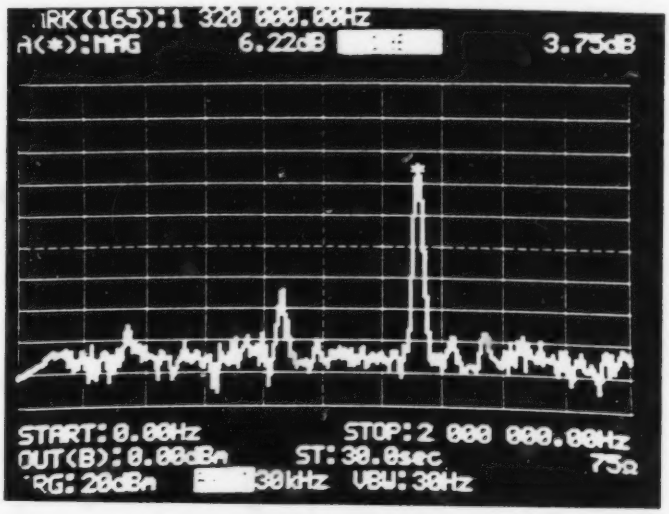

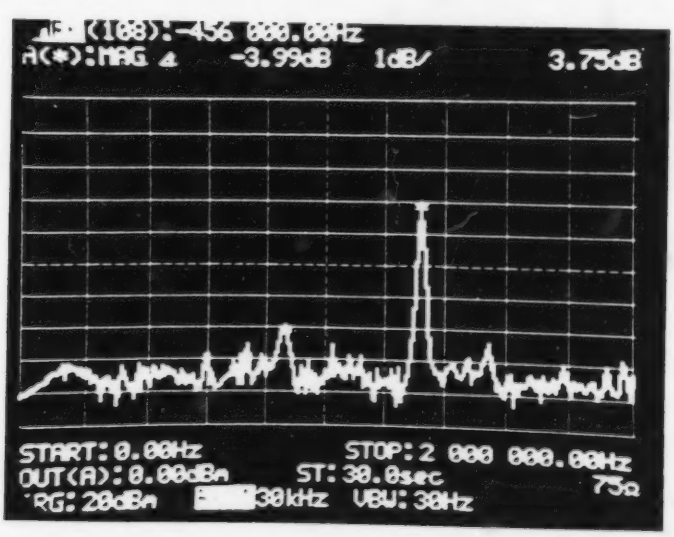

Figure 12. Frequency spectra of signal after passing through 4.2cm and 13cm respectively

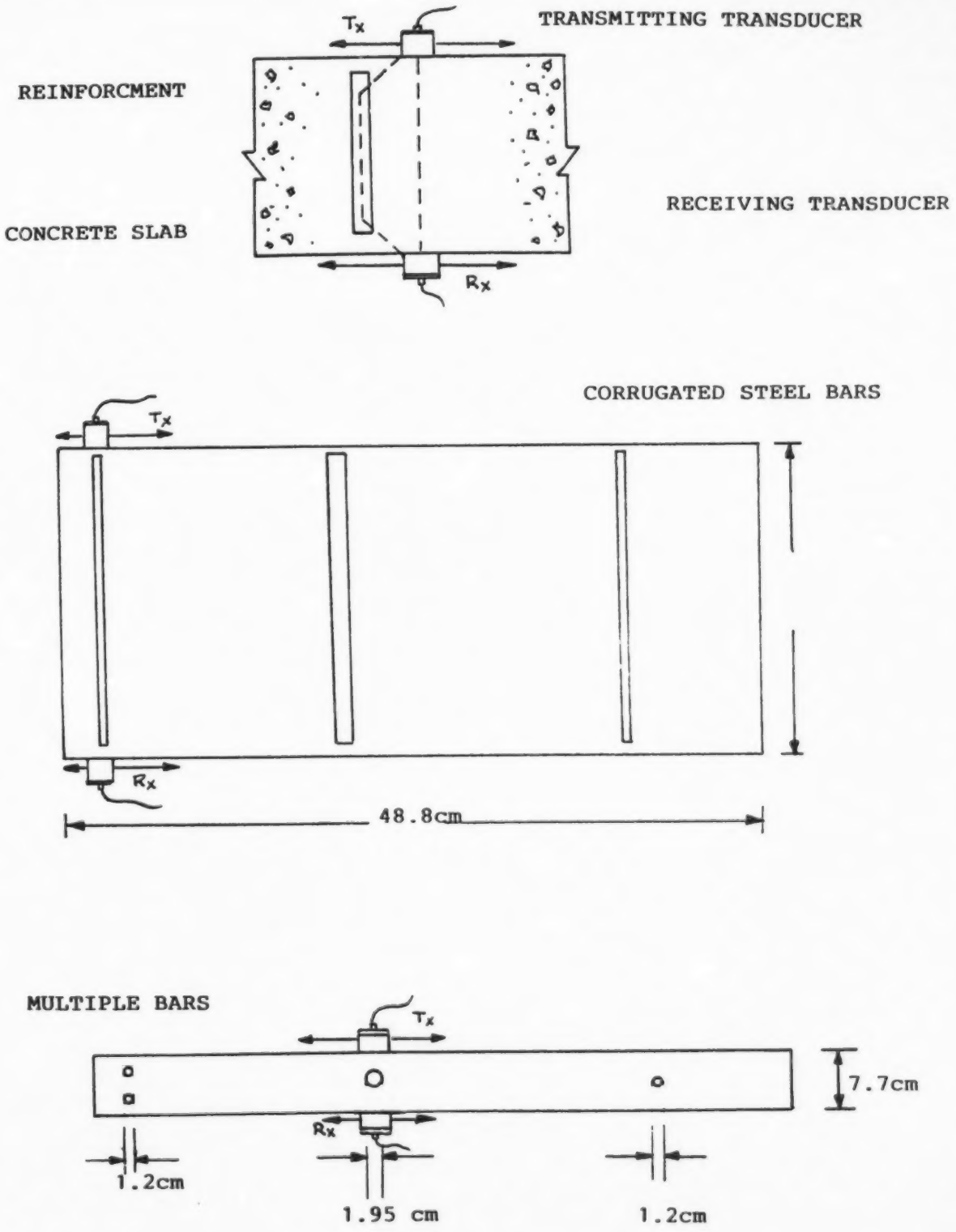

Figure 13. Experimental arrangement for rebar monitoring

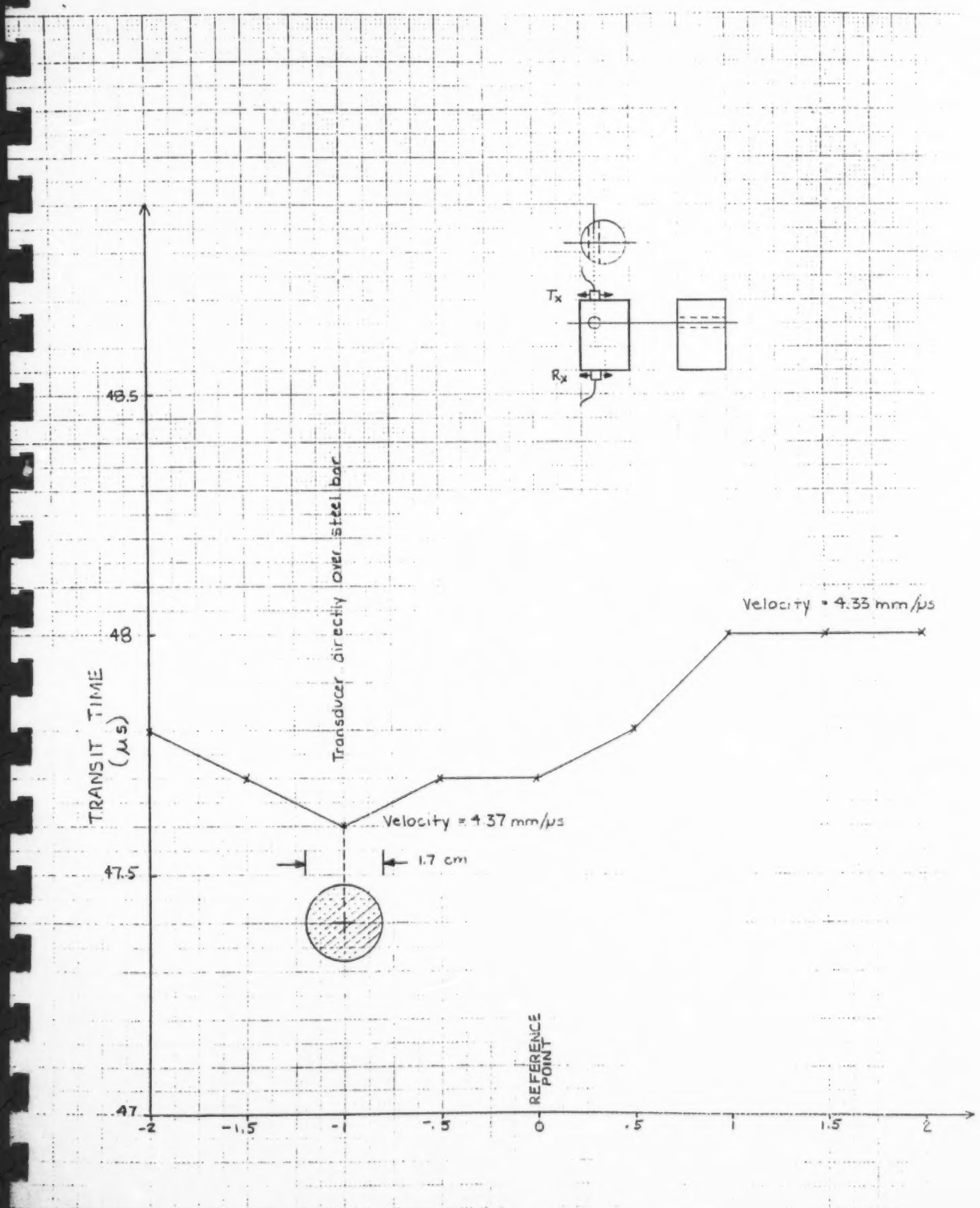

Figure 14. Velocity of concrete in vicinity of reinforcement bar

Figure 15. Histogram - Detection of crack with and without presence of water

Maximum crack thickness = 0.056cm
Test sample C1

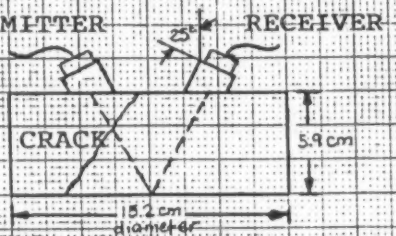

TRANSDUCER SEPARATION = 8.5cm

Vrec (mVp-p)

RECEIVED AMPLITUDE LEVELS

170
160
150
140
130
120
110
100
90
80
70
60
50
40
30
20
10

WET SAMPLE

WET SAMPLE

DRY SAMPLE

DRY SAMPLE

CRACK

NO CRACK

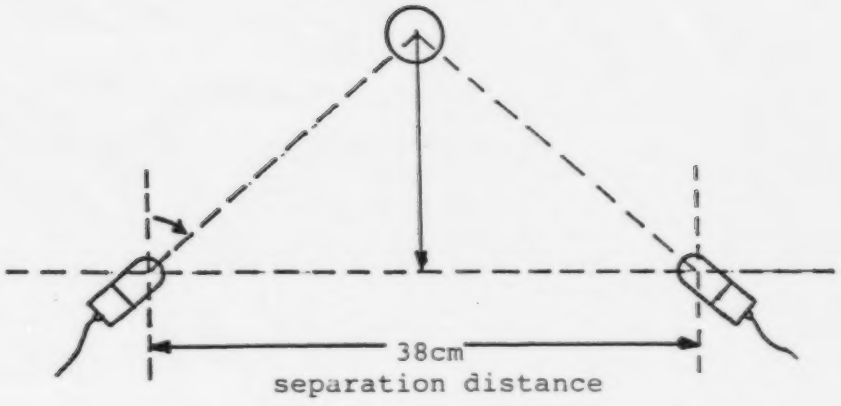

$$1 = \frac{x}{\text{separation}/2} \qquad \therefore\ x = \text{separation}/2$$

Figure 16a. Geometry of transducer placement to test vertical hole

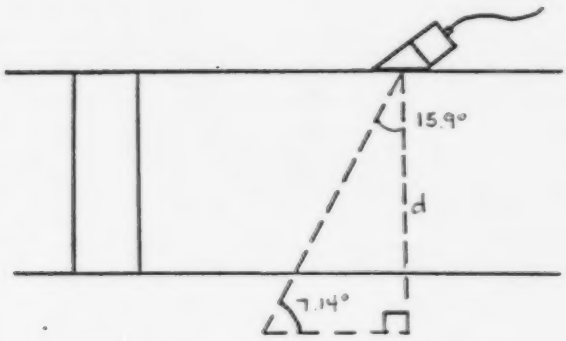

$$\text{TAN } 15.9° = \frac{18.8\text{cm}}{d}$$

$$\therefore\ d = 3.51 \times 18.8\text{cm}$$

$$= 65.988\text{cm}\ (25.97\text{ inches})$$

$$= 2.1\text{ feet}$$

Figure 16b. Projection of actual sound path

Maximum signal observed was 30mVp-p

TOF (time of flight) = 160.6us

1st peak = 530.5us
2nd peak = 1183us
3rd peak = 1783us
4th peak = 2446us
5th peak = 3033us

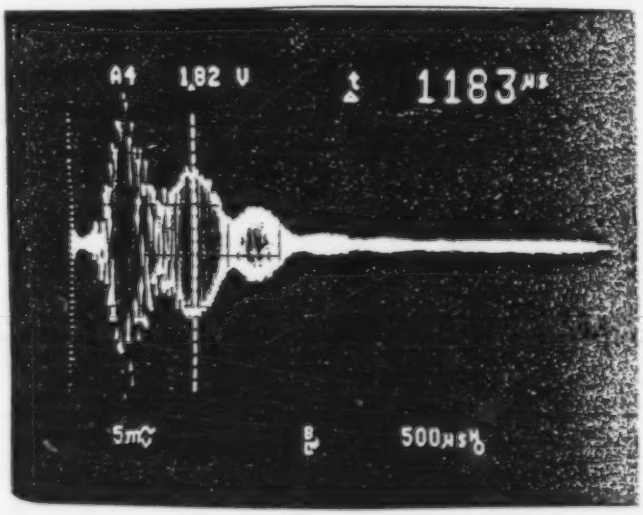

Figure 16c. Reflection of signal from hole

Figure 17. Change of reflected compressional wave amplitude vs change in distance of transducers from crack.

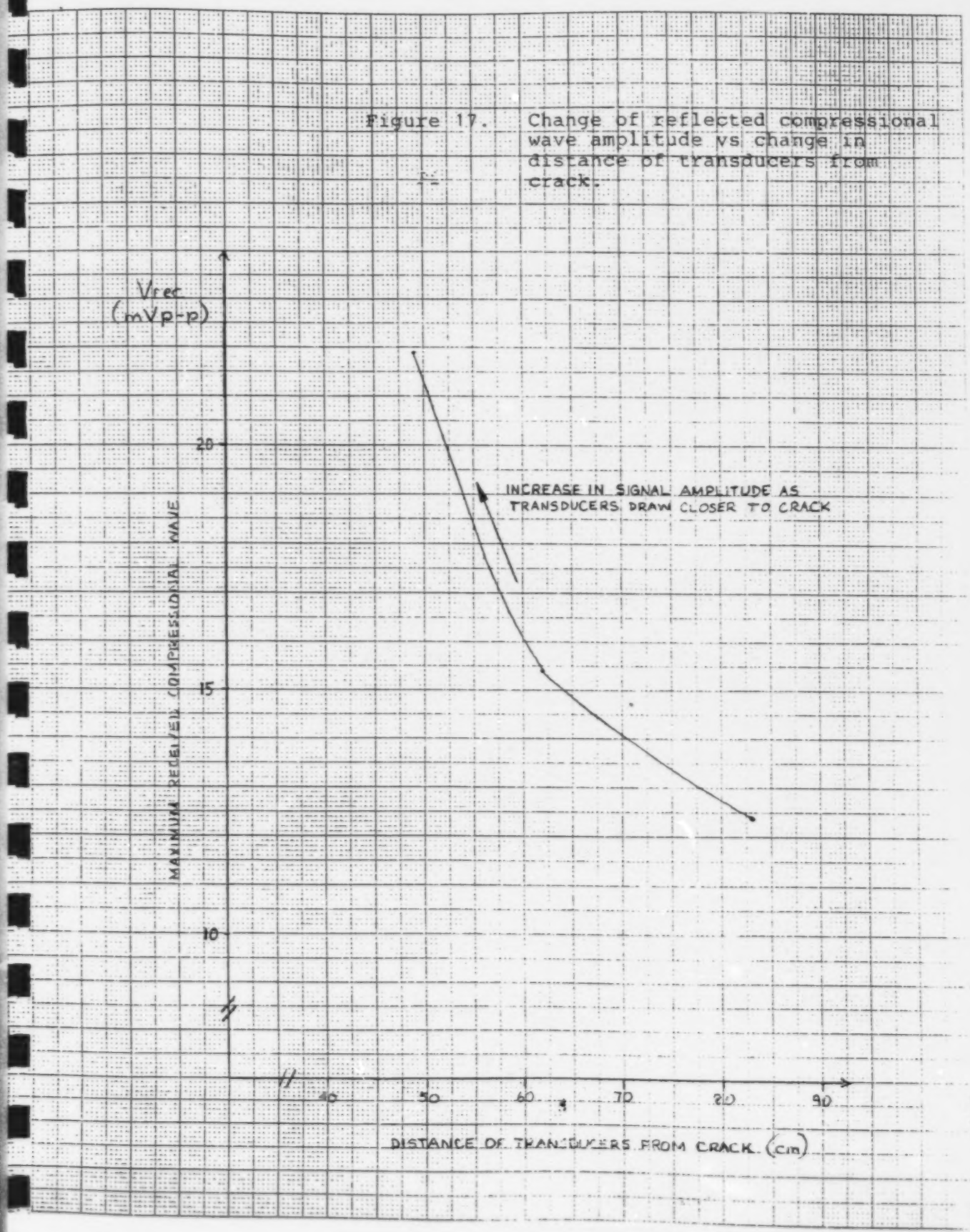

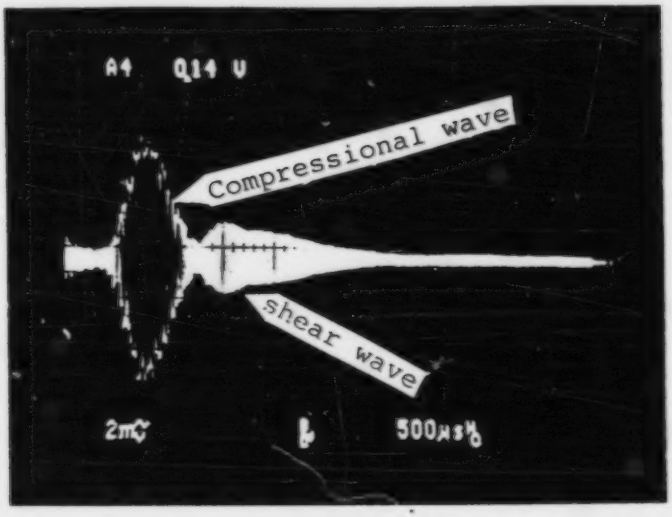

Figure 18a. Reflection of flaw at a separation distance of 72cm with a 25° angle wedge

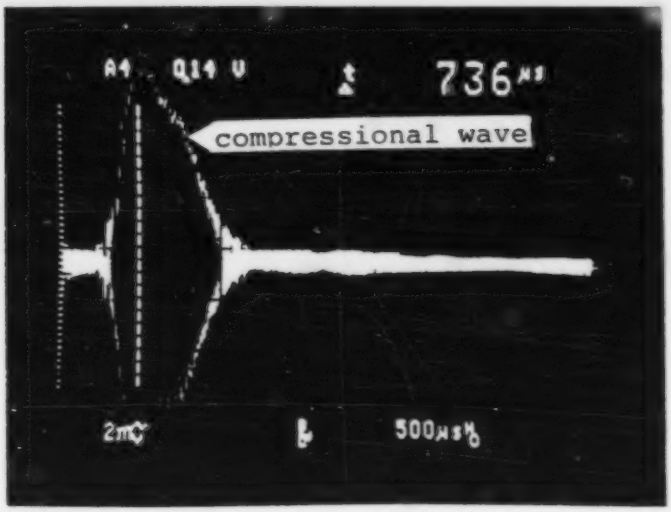

Figure 18b. Reflection of flaw at a separation distance of 72cm with a 45° angle wedge

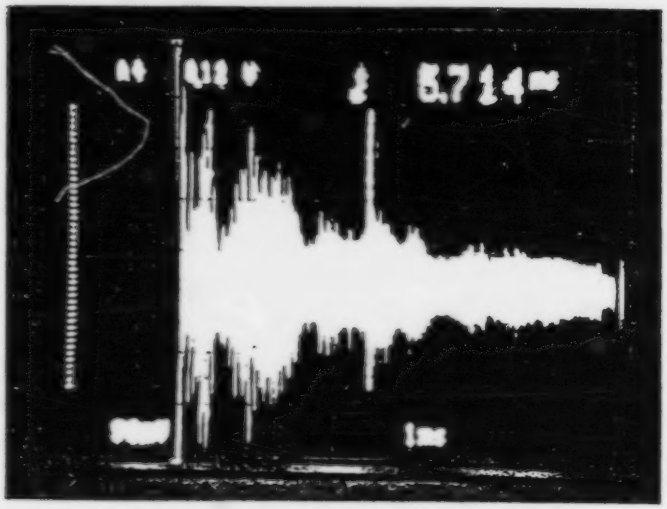

Maximum signal at 3094 us showing depth
of crack at 22.6 feet.

Figure 19 Strong crack indication at 22 feet from surface

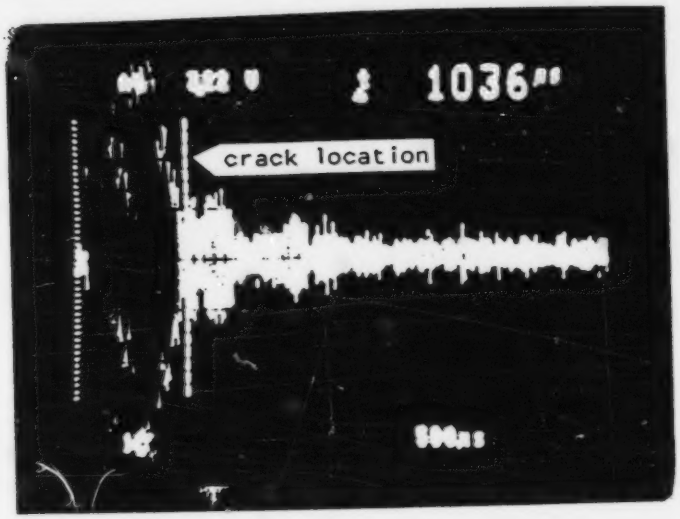

Figure 20a. TOF = 1036 us
Depth of crack = 4.3'

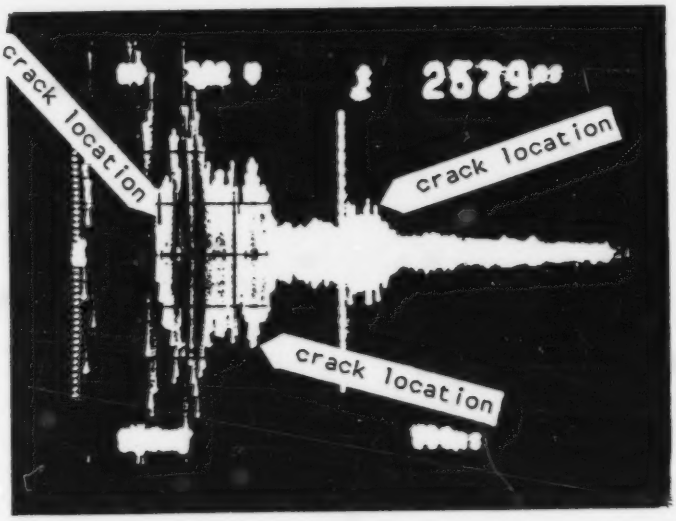

Figure 20b. TOF = 800 us, Depth = 4.9'
TOF = 1550 us, Depth = 9.4'
TOF = 2539 us, Depth = 15.4'

Examples of different crack indications in old concrete structures

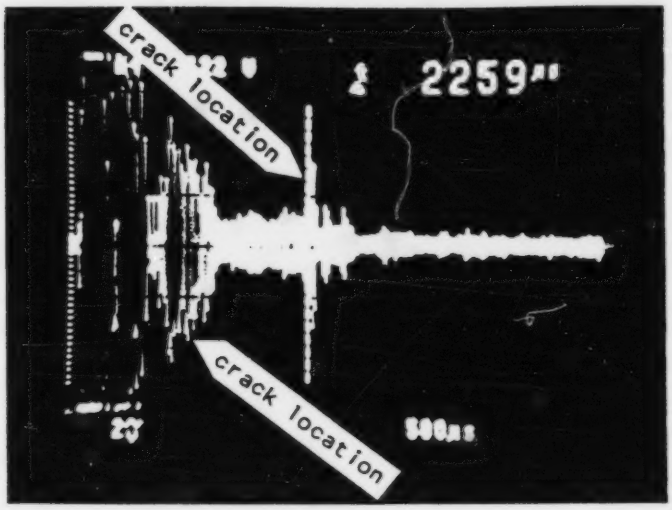

Figure 20c. TOF = 897 us, Depth = 5.4'
TOF = 2259 us, Depth = 13.7'

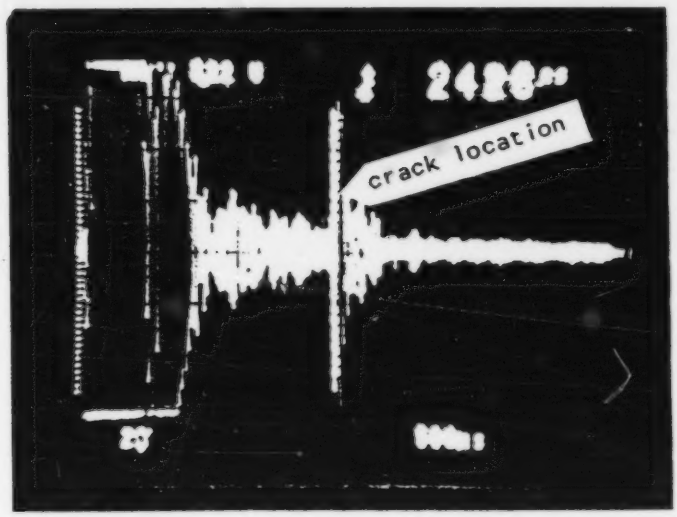

Figure 20d. TOF = 2428 us
Depth of crack = 14.74'

Examples of different crack indications
in old concrete structures

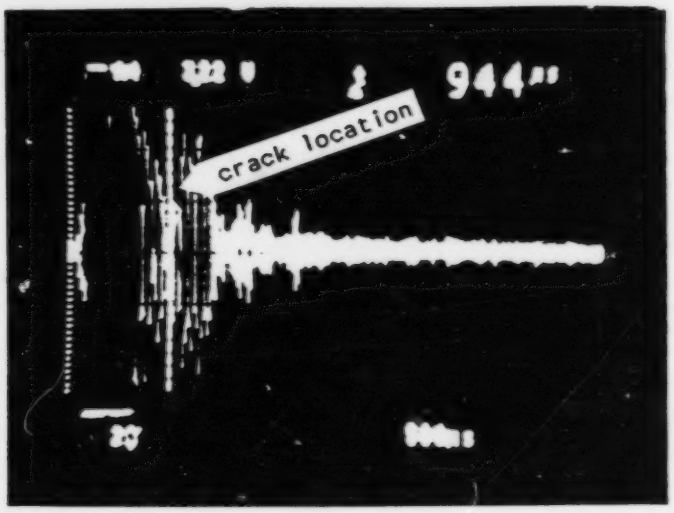

Figure 21 Typical pulse-echo RF waveform signal showing surface wave and following compressional wave echoes from the crack

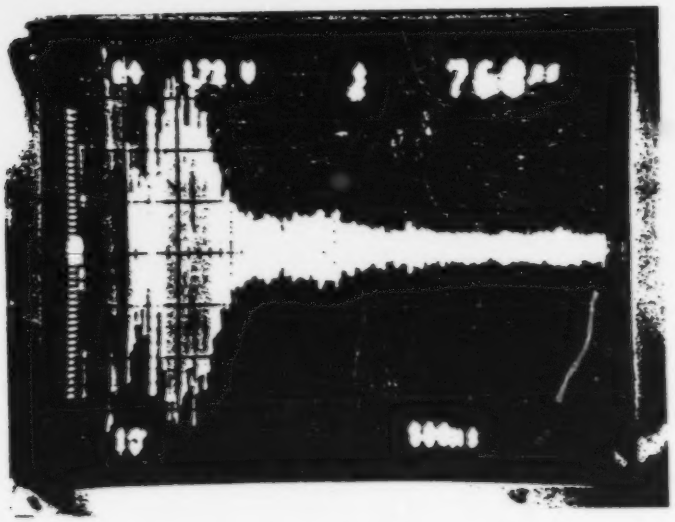

Figure 22 Echo signal discernable within surface wave deadzone pulse

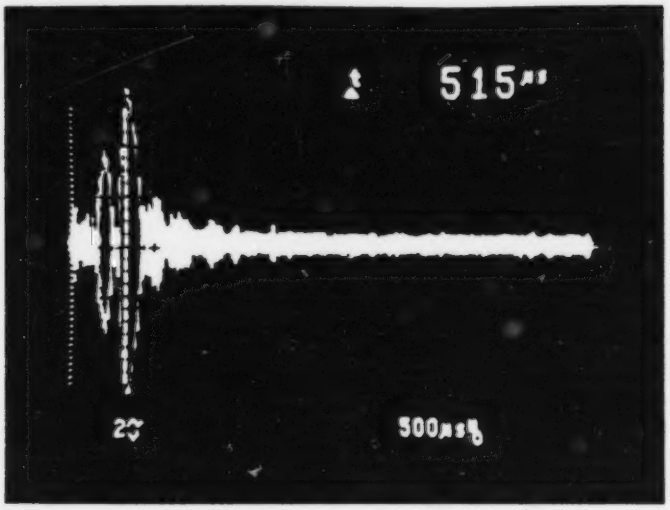

Figure 23a. Pulse-echo signal of crack in newer concrete. Notice shorter echoes and high S/N ratio.

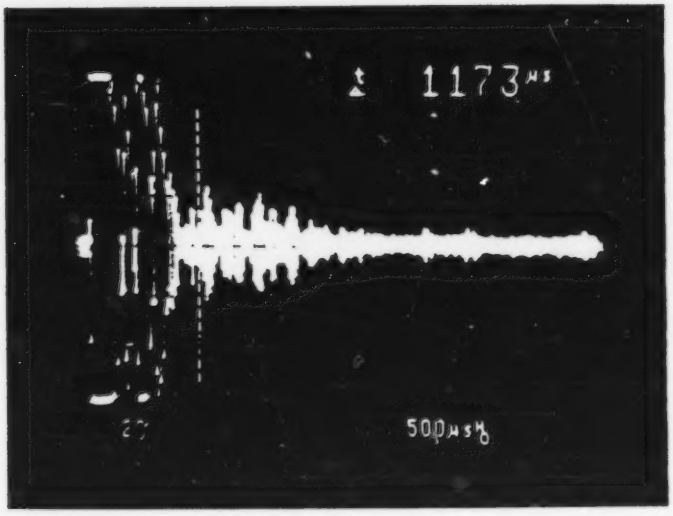

Figure 23b. Pulse-echo signal of crack in newer concrete. Notice shorter echoes and high S/N ratio.

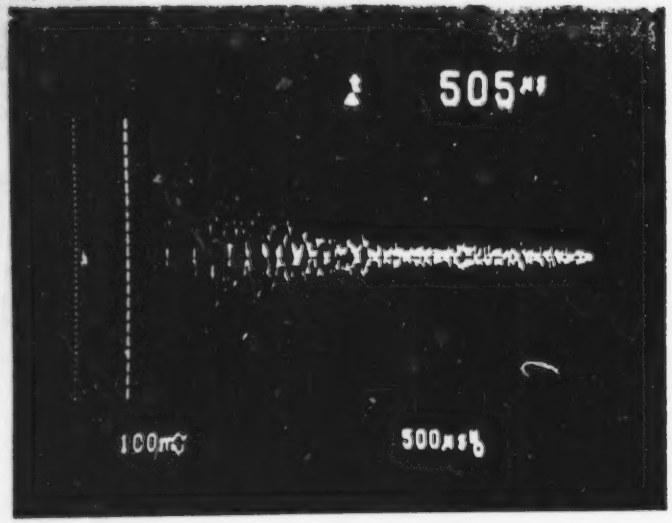

Figure 24a

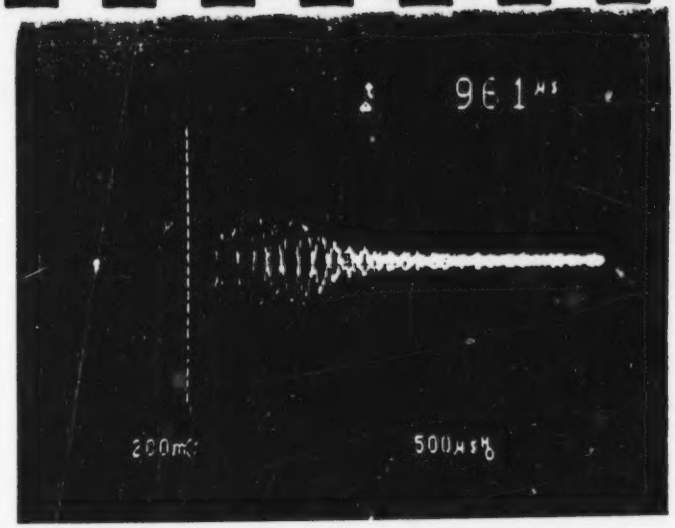

Figure 24b.

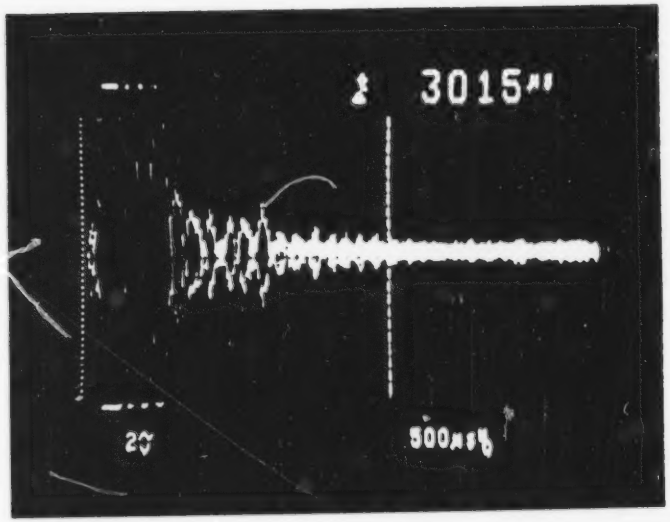

Figure 24c.

Examples on reinforcing bar echoes evenly spaced in structures.

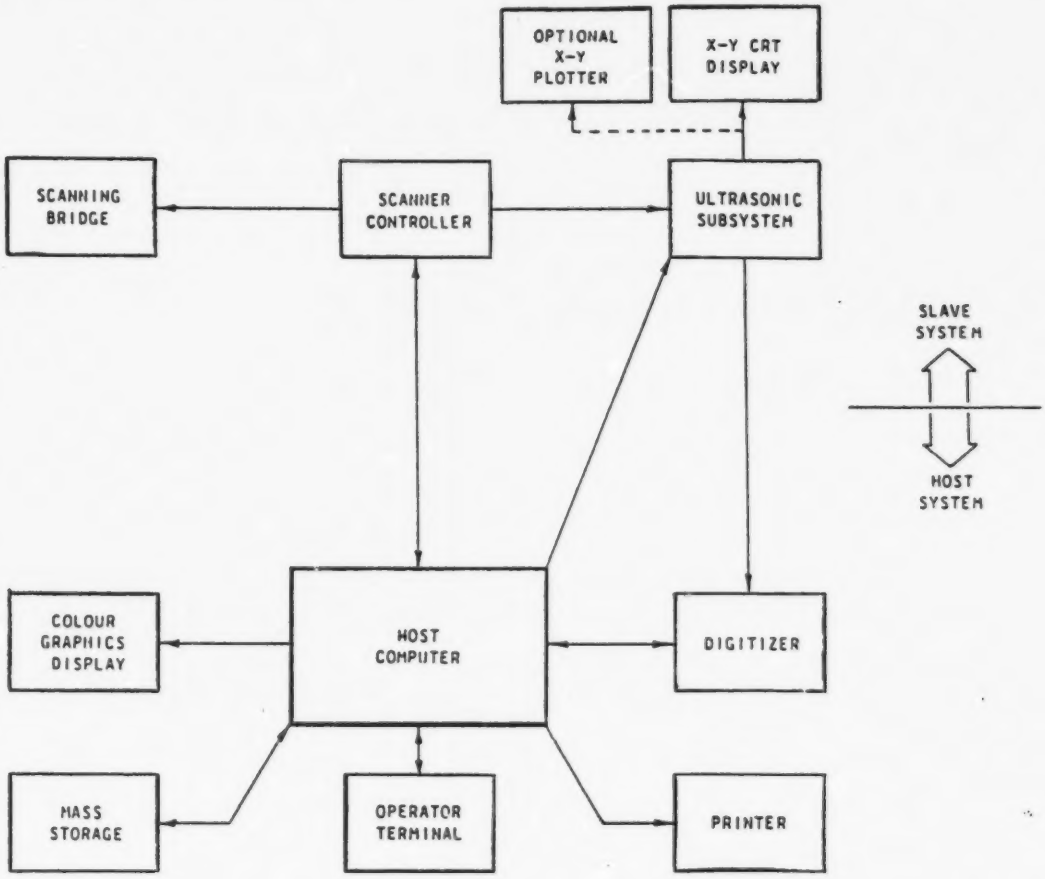

Figure 25. Block diagram of digital data acquisition

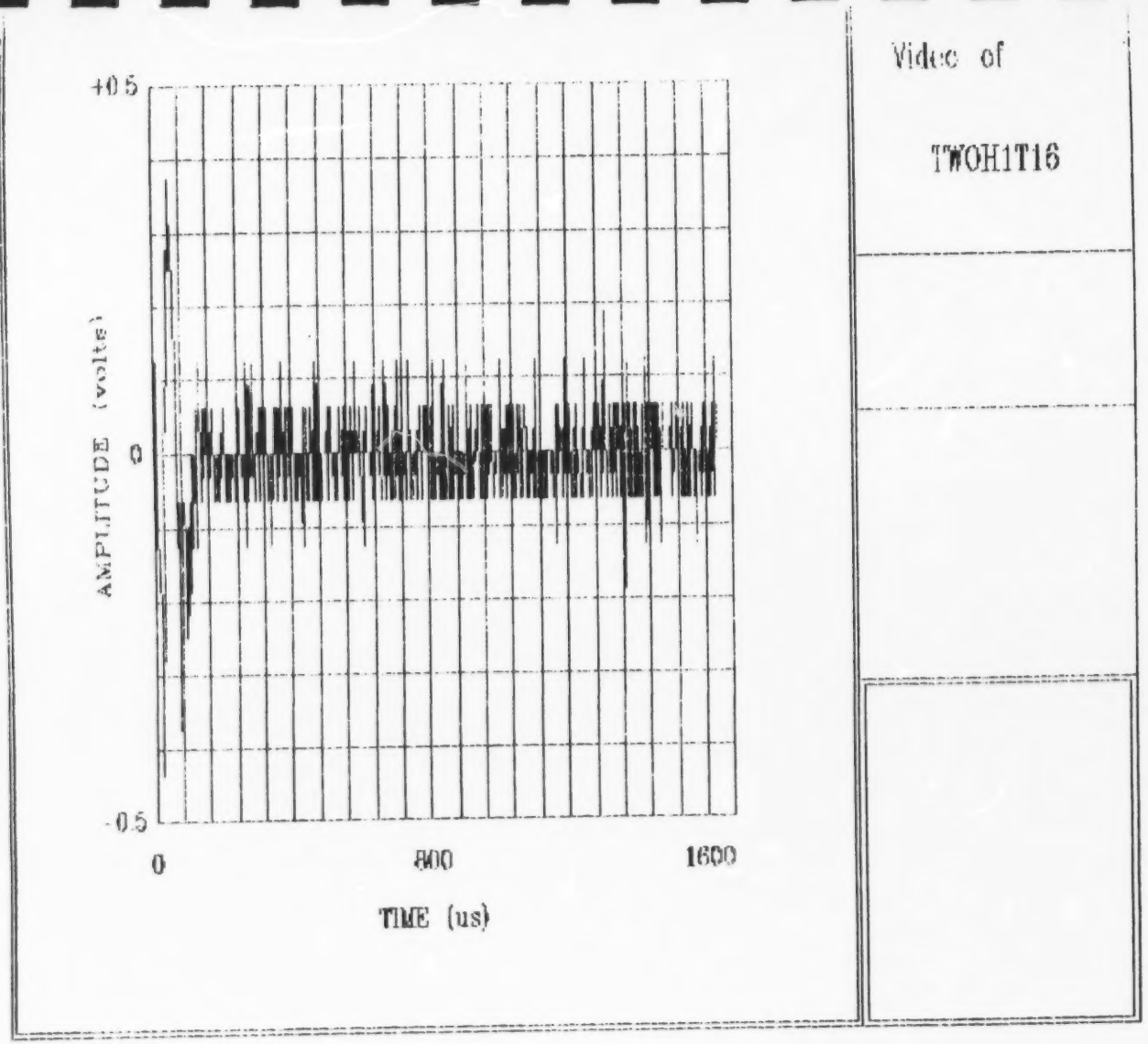

Figure 26 Digitized waveform of a pulse through SMPL 2H

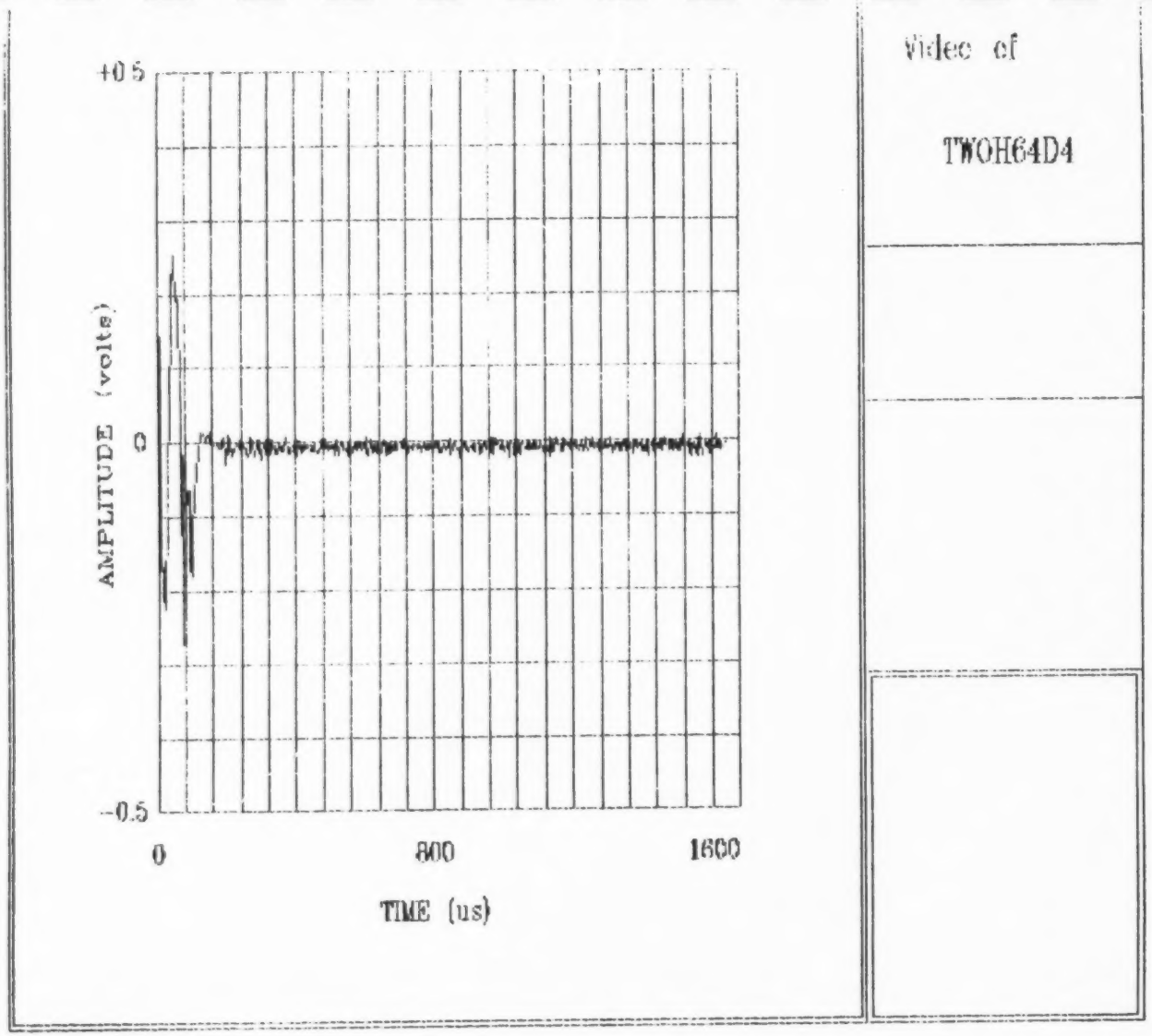

Figure 27 Digitized waveform of a pulse after averaging of 64 samples. Notice increased S/N ratio.

APPENDIX B - SPECIFICATIONS FOR THE PORTABLE UNIT

Specifications describe the instrument's features and methods by which the constraints of concrete inspection.

The system is composed of five major divisions:

1) Ultrasonic transducer
2) Ultrasonics
3) Microcomputer
4) Software
5) Controls/Display

Ultrasonic Transducer

The transducer provides the means by which ultrasonic signals may be injected into and recovered from the concrete test piece. The design of the transducer is critical. The impedance of the crystal elements must be matched mechanically to the test piece and electrically to the ultrasonic circuitry. The transducer must be damped to prevent its oscillation from interfering with reflected echoes. A number of transducers at different resonant frequencies sizes and sensitivities will be provided for different applications.

Ultrasonics

The circuitry for the ultrasonics will generate the excitation pulse for the transducer, and will perform signal processing of the returned echoes. The ultrasonics consists of a pulser, a receiver with logarithmic amplifier and a digitizer.

Microprocessor Controller

The microcomputer, operating with the software, will control all the functions of the instrument. This will include data acquisition, signal processing, menu selection etc.

Software

The software will be written to perform 4 major tasks: transit time measurement, signal processing and calculation, fault condition monitoring and data input/output coordination. The software will also coordinate input data for instrument operating parameters and will output information to the user or to permanent storage.

Controls/Display

The controls and display will allow the operator to change operating parameters for different measurement procedures. These procedures will be menu driven and a CRT will display stored data. The overall block diagram is shown in Figure A3.

The superiority of our approach is that ultrasonic reflections from internal defects or external boundaries can be monitored and setting of the instrument is optimized by the operator.

Another advantage of our approach is the burst driving capability to deliver high power to a transducer, thus increasing the penetrating power into the test piece of large depth.

Pulser

The high voltage excitation required for the transducer is generated by the pulser. The voltage produced is 1000V in amplitude in a 50 load, and rises to this level in nanoseconds. Thus, the broadband frequency spectrum will cause a resonant oscillation in any given transducer (Figure A1).

Tone Burst Generator

A burst driving pulser will also be incorporated into the system to provide increased penetration power of the transducer. The burst generator will provide variable repetition rate of burst, variable burst length, and a variable burst frequency which may be adjusted to achieve maximum response of the transducer (Figure A2).

Receiver

The received echo signals of the ultrasonic transducer and the resulting electrical signals will be small in uV levels. The receiver will amplify the echo signals to a more useable level for digitization and signal processing.

Digital Converter

As an interface between the ultrasonics and the microcomputer, the digital converter will provide the digital conditioning and gate generation for 'start' and 'stop' pulses. These pulses will accurately provide a transit time reading of the backwall echoes.